ONE-DIMENSIONAL TRANSIENT FLOW IN PIPELINES

MODELLING AND SIMULATION

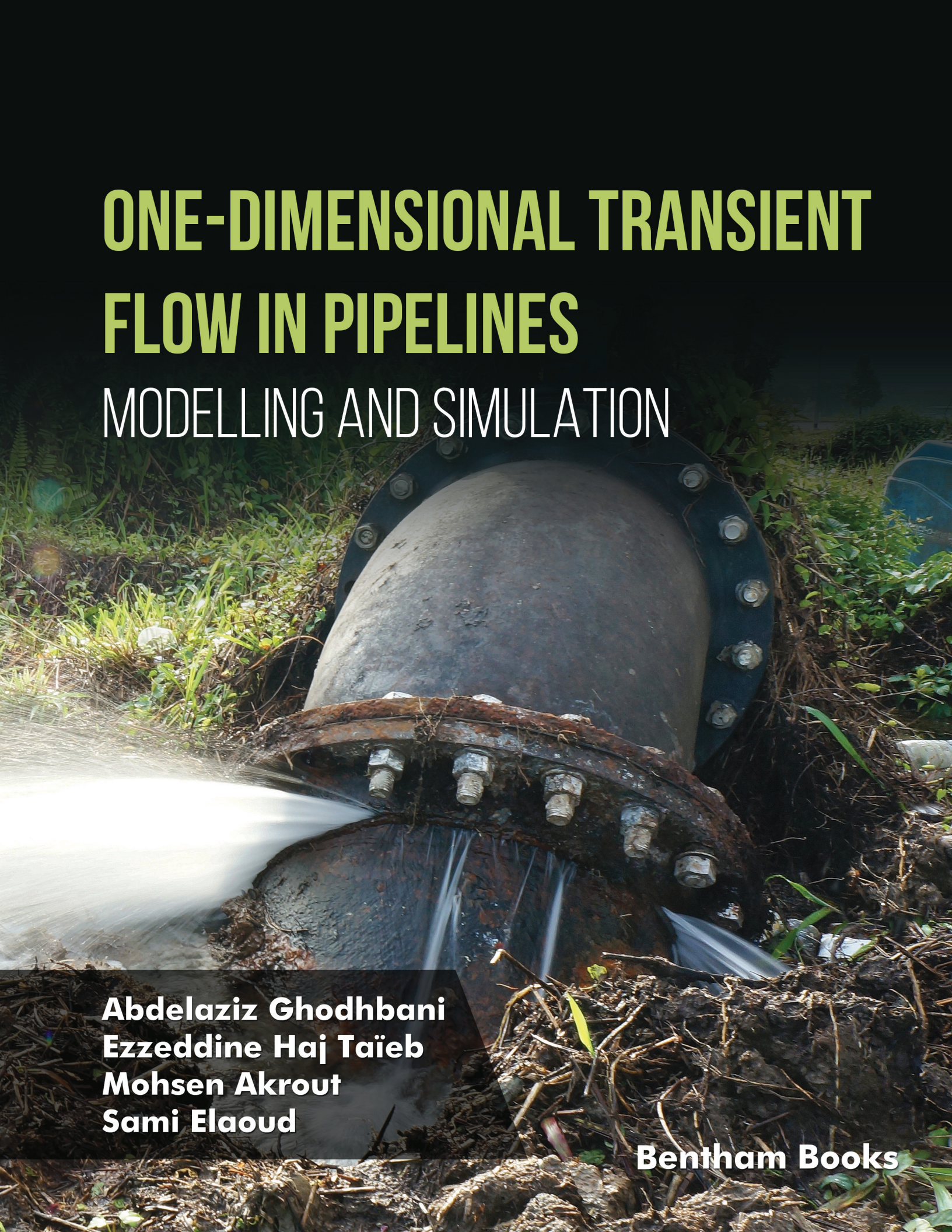

Abdelaziz Ghodhbani
Ezzeddine Haj Taïeb
Mohsen Akrout
Sami Elaoud

Bentham Books

One-Dimensional Transient Flow in Pipelines Modelling and Simulation

Authored by

Abdelaziz Ghodhbani
National Engineering School of sfax
University of Sfax
Tunisia, Africa

Ezzeddine Haj Taïeb
National Engineering School of sfax
University of Sfax
Tunisia, Africa

Mohsen Akrout
National Engineering School of sfax
University of Sfax
Tunisia, Africa

&

Sami Elaoud

National Engineering School of sfax
University of Sfax
Tunisia, Africa

One-Dimensional Transient Flow in Pipelines Modelling and Simulation

Authors: Abdelaziz Ghodhbani, Ezzeddine Haj Taïeb, Mohsen Akrout and Sami Elaoud

ISBN (Online): 978-981-5123-76-0

ISBN (Print): 978-981-5123-77-7

ISBN (Paperback): 978-981-5123-78-4

First published in 2023.

need for a court order if at any point you breach any terms of this License Agreement. In no event will any delay or failure by Bentham Science Publishers in enforcing your compliance with this License Agreement constitute a waiver of any of its rights.

3. You acknowledge that you have read this License Agreement, and agree to be bound by its terms and conditions. To the extent that any other terms and conditions presented on any website of Bentham Science Publishers conflict with, or are inconsistent with, the terms and conditions set out in this License Agreement, you acknowledge that the terms and conditions set out in this License Agreement shall prevail.

Bentham Science Publishers Pte. Ltd.
80 Robinson Road #02-00
Singapore 068898
Singapore
Email: subscriptions@benthamscience.net

CONTENTS

FOREWORD

The authors have written this book based on their research in computational fluid mechanics (CFD), specifically on transient fluids. The mathematical formulation of the physical phenomena occurring in fluid pipes, the use of the method of characteristics (MOC) as a tool to solve the governing equations of the numerical models and the coding strategy of these numerical models into a CFD tool are three difficult but essential steps for any fluid mechanics' research study. These steps are well presented and detailed in this book.

The book is written in simple English and the Mathematical and Numerical formulations of the physical problems are reasonably explained. The numerical code algorithms are detailed in appendices. In brief, the book provides a simple one-dimensional method to predict what happens exactly in a fulfilled straight pipe when water hammer and cavitation phenomena occur therein. Finally, this book will surely help readers to develop their modelling skills in fluid mechanics.

Hab. Eng. Ridha ENNETTA
Mechanical Engineering
University of Gabes
Tunisia
Africa

PREFACE

Hydraulic transients also referred to as fluid transients or water hammer usually cause leakage and rupture of pipelines. Since pressure rises are responsible of these accidents, engineers, and researchers are always trying to predict the pressure history in given hydraulic plants. This purpose requires in fact accurate modelling and calculation. Perhaps, readers who are interested in fluid mechanics have met at least one complicated situation revealing water hammer. Indeed, this phenomenon is not simply solved; partial differential equations are present, where the continuity equation and the equation of motion are used. Moreover, water hammer results in transient cavitation (vaporous cavitation and gaseous cavitation), which is a combination of thermodynamic and hydraulic phenomena. Transient cavitation is destructive for hydraulic plants. The entire content of this book is a mathematical and numerical study of transient cavitation in pipelines. The emphasis is made on coupled modelling and its numerical calculation. During several years of research, the author has focused on the accuracy of the numerical result. Different models, methods and assumptions are tested in order to be close to the experimental result. These are detailed in the present book. The simulation of vaporous cavitation and gaseous cavitation by use of coupled modelling is attempted to be useful. The improvement of the numerical simulation leads to the improvement of the design of pipes in hydraulic engineering. Two types of pipelines will be considered: the quasi-rigid elastic pipelines (metal and concrete) and the VE pipelines (polyethylene). Experimental results from the literature is used to validate the proposed models. The first chapter which is a review of the literature describes the main previous works on fluid transient in pipelines. The mathematical formulations of water hammer and cavitation are detailed in the second chapter. The mathematical modelling detailed concerns water hammer and cavitation. The numerical resolution of the various models using the MOC is presented in the third and the fourth chapters. Chapter 3

describes the numerical resolution proposed for the water hammer models, while the numerical modelling of transient cavitation is the subject of the fourth chapter. The results of the numerical simulation of water hammer and cavitation in elastic pipelines are introduced and discussed in the fifth chapter where the WSA scheme is highlighted. The final chapter is reserved for the simulation of water hammer and cavitation in VE pipeline.

Abdelaziz Ghodhbani
National Engineering School of Sfax
University of Sfax
Tunisia, Africa

Ezzeddine Haj Taïeb
National Engineering School of sfax
University of Sfax
Tunisia, Africa

Mohsen Akrout
National Engineering School of sfax
University of Sfax
Tunisia, Africa

&

Sami Elaoud
National Engineering School of sfax
University of Sfax
Tunisia, Africa

INTRODUCTION

Hydraulic networks, such as water supply systems, irrigation networks, hydropower stations, nuclear power plants, petroleum plants and cooling systems in thermal power plants are usually affected by strong pressure variation due to hydraulic transients. This is a spectacular form of unsteady flow in liquid-filled pipe systems usually referred to as “water hammer”. This phenomenon is mostly due to the sudden closing and opening of valves, starting, and stopping (or failure) pumps and turbines. The kinematic energy of the liquid transforms to a pressure energy following the accident. The large transient pressure variations resulting from the water hammer may damage the pipe systems and their components (junctions, valves, elbows, pumps, *etc*.). Water hammer can also lead to severe low pressures usually resulting in distributed cavitation or localized column separation. The condensation of vapour in case of vaporous cavitation or the dissolving of gas in case of gaseous cavitation involves strong collapses and subsequently hight pressure surges. Noting that the concept of “water hammer” refers to “transient without cavitation” while “transient cavitation” is a special case of fluid transient.

Cavitation is known in hydraulic engineering as the most dangerous accident for pumps, turbines, and pipelines. Prevention should be taken at critical points to avoid damage and leakage. The simplest is to minimize the flow velocity by making a wise choice of diameter. Also, prevention can be done by extending the closing times of automated or motorized valves by means of springs, dampers or magnetic brakes and the stopping time of the pumps using the flywheels. The use of anti-ram chambers with compressed air mattresses can be as effective. Another technique is to add an equilibrium chimney to the pipes of high calibre supply.

The location of critical points as well as the choice and the dimensioning of protective components require preliminary study and rigorous numerical simulation. To achieve this, mathematical modelling is necessary. All physical and dynamic parameters affecting the water hammer are taken into account: densities, modulus of compressibility of the fluid, modulus of elasticity of the pipe, initial flow velocity, initial pressure, *etc*. The mechanical behaviour of the pipe, whether elastic quasi-rigid (metals and concretes) or viscoelastic (like PVC), is also considered. The steady state defines the initial conditions of the problem whereas the physical boundary conditions of the hydraulic system are introduced into the model. In addition, fluid-structure interaction (FSI) should be considered because of the existence of three dynamic coupling modes namely: (i) fluid-wall friction (friction coupling), (ii) pipe expansion and contraction (Poisson coupling) and the

inertia force of the pipe and components (junction coupling). If FSI is ignored, the calculations provide only two fluid variables namely the pressure "p" (or piezometric head "H") and the velocity "V" (or discharge "Q"). If FSI is considered, then several structural responses can be obtained besides the above fluid characteristics, such as the displacement, the pipe velocity, stresses, and strains.

There are two mathematical considerations to describe hydraulic piping systems under various hydraulic conditions [1]. The first one concerns the elastic models or water hammer models that consider fluid compressibility and pipe-wall mechanical characteristics. The pipeline is assumed to be elastic (or quasi-rigid). The elastic models are used to describe water hammer, in other word, fast changes in flow conditions, such as valve manoeuvres, pumps start-up or shutdown, or pipe bursts. For these models, the flow is usually considered one-dimensional and described by a system of differential equations. The second one deals with the rigid models or lumped models, which are valid only when the flow conditions vary slowly in time. For these models, the fluid and pipe compressibility effects can be neglected, and the fluid can be described by a rigid column. The system of hyperbolic differential equations, typical of elastic models, is simplified to a set of ordinary differential equations that can be solved by Modified Euler Method or Runge-Kutta Methods. The rigid models can be efficient for slow variations of flow, such as the increase of consumption in peak hours, in which it is important to account for the inertia of the system. The transition between the unsteady compressible flow (elastic model) and unsteady incompressible flow (rigid model) is set by the ratio between the total internal energy change and the total kinetic energy change [1].

There are various FSI models for water hammer in the literature, but the four-equation model is the most suitable among them because of its simplicity and reliability. Only axial vibration of the pipe is considered in this model; the circumferential and radial motion are ignored in much research.

Regarding viscoelastic (VE) modelling, numerous research focuses are taken on this field. The VE behaviour is usually studied by considering mechanical element to describe it; the spring for elastic response and the dashpot for viscous response. Usually, the generalized Kelvin-Voight model is used to describe VE behaviour. Fluid transient in VE pipelines, such as polyethylene can be predicted thanks to the classical VE model, in which the retarded circumferential strain is calculated. Although the important effect of the pipe material on the pressure history during fluid transient, FSI models (four-equation models) are rarely used for water

hammer prediction in VE pipes. Mostly, unsteady friction (UF) is ignored because friction damping VE can be neglected against VE damping.

The cavitation models obviously differ from water hammer models because of the existence of the two-phase liquid-vapour flow. The void fraction of vapour in the mixture is introduced in the governing equations. Cavitation models are very numerous, but they can be grouped into two large families: the column separation models, for example the discrete vapour cavity model (MCVD) and the discrete gas cavity model, and the distributed cavitation models. Regardless the model type, dynamic coupling can be included in the governing equations, but it can be observed that FSI is rarely introduced in cavitation models in the literature [2]. Nevertheless, the prediction of structural responses accompanying fluid transients with cavitation requires coupled analysis in which FSI should be accurately described, especially in case of axial freely moving pipes. In practice, it is impossible to carry out hydraulic plants with entirely rigid pipelines.

In order to obtain accurate results, water hammer calculations in pipelines require the use of appropriate numerical method. The method of characteristics (MOC) is the most preferred one because the wave-speeds are constant in time (no dispersion). The majority of the commercially available water hammer software packages use the MOC. The numerical schemes are usually based on linear space or linear time interpolations. Nevertheless, since interpolation results in errors, researchers use the wave-speed adjustment scheme (WSA), which is more flexible and more efficient. The Finite Element Method (FEM) provides great flexibility in handling variable-size elements in different properties. The method consists firstly in substituting a shape function into the differential equations. Then the residual (difference between the shape function and the exact solution) is multiplied by a weighting function to obtain a weighted residual. After that, the FEM attempts to force this weighted residual to zero in an average sense. The choice of the weighting functions can be obtained with different schemes, namely the Galerkin scheme and the Petrov-Galerkin scheme. Another way is to combine two numerical methods: The FEM and the MOC. The new method is called FEM-MOC. The former is suitable for structural calculation (pipe), whereas the latter is preferred for the fluid calculation. However, this technique is not preferred than the full MOC. The Finite Difference Method (FDM) is efficient in calculation of distributed cavitation models because the pressure wave-speed is no longer constant. For implicit schemes, the FDM has the advantage of stability for large time step. However, the time and the storage requirement are increaded. Therefore, implicit schemes are not suitable for wave propagation problems because they entirely distort the path of propagation of information. Recently,

hyperbolic problems are usually solved by explicit schemes, such as MacCormak and Lax-Wendroff schemes. The Finite Volume Method (FVM) is also used for hyperbolic problems, such as gas dynamic, shallow water waves and water hammer flows. The first-order based Godunov scheme is widely used for this method. It is very similar to the MOC with linear space-line interpolation.

From the foregoing description, some recommendations can be established for calculation of hydraulic transient. First, one should select appropriate model and appropriate numerical method. Secondly, some assumptions are needed for easier calculations and obviously there are some limitations for such assumptions. Thirdly, the dynamic coupling mechanisms complicate the models, and it becomes unnecessary to use them unless they lead to eventual improvement of the solution, or when structural responses prediction is needed. Finally, the computer code should be efficient otherwise, any numerical error involved cannot be easily avoided. Recently, several computer software are developed for computational fluid dynamics (CFD), and fluid transient problems represent the most important application for them. The most popular CFD products are Matlab and Ansys Fluent. The majority of reviewers stated that Matlab is designed for numerical computing and visualization but is not suited for intensive computation. However, Ansys Fluent is essentially directed for modelling and simulation thanks to its efficient and automated structured meshing. In this work, numerical computations of numerous variables is needed, all calculations are hence performed by use of Matlab through implementation of several codes written by the present authors.

In this work, a coupled modelling and numerical calculation of fluid transient in pipelines is proposed. The reservoir-pipe-valve system (downstream valve system) is mainly used in defining boundary conditions of the problems. The emphasis is made on cavitation (vaporous cavitation and gaseous cavitation), its effect on the pressure history and especially on the structural responses. Water hammer and cavitation models from the literature will be used in new coupled formulation that considers the effect of FSI on the numerical solution. Friction coupling effect will be tested by comparison between steady friction (SF) and UF. Poisson coupling will be investigated by use of the four equation model. To introduce the junction coupling, axial free-moving valve will be considered and compared to the fixed valve case. Elbows systems lead to higher junction coupling and additional lateral vibration of the pipe. Such configurations are more complicated and may be investigated in next works. The objective is to improve water hammer understanding associated with local column separation.

NOMENCLATURE

Abbreviations

4EM	Four-equation Model
4EFM	Four-equation Friction Model
4EVEM	Four-equation Viscoelastic Model
BPA	Benchmark Problem A
CCC	Constant creep-compliance
CWS	Constant wave-speed
CFD	Computational Fluid Dynamics
DVCM	Discrete Vapour Cavity Model
DGCM	Discrete Gas Cavity Model
FDM	Finite Difference Method
FEM	Finite Element Method
HDPE	Hight Density Polyethylene
HGL	Hydraulic Grade Line
MOC	Method of Characteristics
QR	Quasi-rigid
RG	Rectangular Grid
SF	Steady friction
SG	Staggered Grid
SLI	Space-line Interpolation
TLI	Time-line Interpolation
UF	Unsteady friction
CCC	Constant creep-compliance
VCC	Variable creep-compliance

VWS	Variable wave-speed
VEM	Viscoelastic Model
VE-DVCM	Viscoelastic Discrete Vapour Cavity Model
VE-DGCM	Viscoelastic Discrete Gas Cavity Model
WSA	Wave-speed Adjustment

Scalars

α	Vapour void fraction / constant
$\forall$	Volume
β	Constant number / coefficient of the Newmark method
δ	Integer equal to 1 or 2
κ	Isothermal compressibility
ρ	Mass density
ψ	Weighing factor
Ω	Number
ε	Axial strain
γ	Pipe inclination / constant
λ	Characteristic direction
μ	Dynamic viscosity
ν	Poisson coefficient / kinetic viscosity
ψ	Weighting factor
σ	Stress
Σ	Constant number
Π	Constant number
Γ	Constant number

τ	Shear stress / retarded time
Φ	Number
Φ	Airy function
ζ	Damping ratio
a, b	Integers
$A, \tilde{A}, \hat{A}$	Cross section
B	Pipeline impedence
c	Anchor coefficient / viscous damping coefficient
C	Celerities / constant number
D	Inner diameter of the pipe
e	Pipe-wall thikness
E	Young's modulus of elasticity
f	Friction coefficient
F	Force / number
G	Number
g	Gravity acceleration
h	Friction head loss / arbitrairy datum
H	Piezometric head
i	Space increment
j	Time increment
J	Creep compliance
k	Constant / number / stiffness coefficient
K	Bulk modulus of the liquid / number
L	Length of the pipe
m	Mass

n	Rational number
N	Number of reaches
p	Pressure
P	Computational point
$q, \tilde{q}, \hat{q}$	discharge
Q	One time-step earlier computational point
R	Radius / two-step earlier computational point
r, R	Radius
t	Time
T	Temperature / period
u	Axial displacement / integration time
V	Celerity
v	Specific volume
W	Weighting function
$Z, \tilde{Z}, \hat{Z}$	Head
z	Axial cordinate

Matrices

A, B	Coefficient matrices of the PDE system
D	Diagonal matrix
I, $\bar{\bar{I}}$	Identity Matrix
M1, M2, M3, M4	Coefficient matrices of the algebraic system for inner sections
R1, R2, R3, R4	Coefficient matrix of the algebraic system at the reservoir
T, S	Transformation matrices

V1, V2, V3, V4	Coefficient matrix of the algebraic system at the valve

Tensors

$\overline{\overline{D}}$	Strain tensor
$\overline{\tau}$	Viscosity stress tensor
$\overline{\overline{\sigma}}$	Cauchy's stress tensor
$\overline{\overline{\overline{\eta}}}$	Orientation tensor

Vectors

k1, k2, k3, k4	Right-hand side vectors of the algebraic system for inner sections
r1, r2, r3, r4	Right-hand side vectors of the algebraic system at the reservoir
v1, v2, v3, v4	Right-hand side vectors of the algebraic system at the reservoir
r	Right-hand side vector of the PDE system
y1	Vector of unknowns of the water hammer models
y2	Vector of unknowns of the column separation models

Subscripts

0	Initial
b	Beat
cav	Cavitation
d	Downstream
e	Elastic

f	Fluid
g	Gas
k	Kelvin-Voight element
l	Liquid
m	Mixture
p	Pipe
v	Vapour
r	Radial coordinate / retarded
s	Steady-state / integration time
T	Isothermal
u	Unsteady-state / upstream
w	Pipe-wall
z	Axial coordinae
φ	Circumferential coordinate

CHAPTER 1

Review of Literature

Abstract: This chapter presents a review of the literature related to fluid transients involving column separation and vaporous and gaseous cavitation in pipelines. Basic concepts are clarified, and the classification of water hammer and cavitation models is presented. The historical development of fluid transients is described. The concept of propagation of pressure pulses at sonic velocity through a straight pipeline is presented.

Keywords: Cavitation; Column separation; Experiment; Water hammer.

INTRODUCTION

Fluid transients in pipelines are an important topic in hydraulic engineering that needs deep studies and research to prevent fluid and pipe responses. Numerous researchers define mathematical and numerical models for this purpose. Others tried to obtain the real behaviour through experiments. In fact, these experiment results serve as references to compare numerical results and validate mathematical models and numerical methods. The aim of this chapter is to focus on the general concepts of fluid transient studies.

FLUID TRANSIENTS

Fluid transients is a large variation in pressure and velocity following an event in the hydraulic system stopping or starting the fluid flow. It is also referred to as water hammer in pipelines. Generally, the phenomenon occurs in full-liquid pipelines and is caused by sudden valve closing, pump stopping and starting, *etc*. As an outcome, fluid transients may lead to severe accident for the hydraulic plants. The concept of fluid transients began in the middle of the nineteenth century by Ménabréa [3, 4] and has continued after the middle of the twentieth century.

Water Hammer Pressure Rise

The water hammer law in a straight pipeline was established by Joukowsky in 1900. The increment of pressure change Δp depends on the increment of flow velocity ΔV *via* [5].

Abdelaziz Ghodhbani, Ezzeddine Haj Taïeb, Mohsen Akrout & Sami Elaoud

$$\Delta p = -\rho_f C_f \Delta V \tag{1.1}$$

with ρ_f is the mass density of the fluid and C_f is the pressure wave-speed. Since $\Delta p = \rho_f g \Delta H$, in which ΔH is the head change, Eq. (1.1) implies [6].

$$\Delta H = -\frac{C_f \Delta V}{g} \tag{1.2}$$

Elastic waves propagate without modification in an infinite isotropic medium but are susceptible to reflection and refraction when they meet a surface separating two different media. Two cases are to consider: (i) When a plane wave propagating in a fluid, normally meets a rigid surface, it is reflected without changing sign: thus, a compression wave is reflected in a compression wave. (ii) When a plane wave propagating in a fluid, normally meets a surface where the pressure remains constant (free surface of a liquid), there is reflection with change of sign: thus, a wave of compression is reflected in a rarefaction wave.

Water Hammer Process

Consider the case of the standard reservoir-pipe-valve-system containing a fluid (*e.g.* water) flowing at the initial velocity V_0 from the reservoir up to the valve. The sudden closure of the valve causes water hammer. By neglecting the friction throughout the pipe, the propagation of water hammer is subdivided into four events (Fig. **1.1**) as follows:

Event 1: At the instant $t = 0$, the valve at the downstream end of the installation is closed. Immediately and close to the valve, the flow rate vanishes. The fluid nearest the valve is compressed to the extra head H and the pipe-wall is stretched (Fig. **1.1a**). As soon as the first fluid layer is compressed, the process is repeated for the next fluid layer. The fluid upstream from the valve continues to move downstream until the compression of the whole fluid column. From an energetic point of view, the kinetic energy of the stopped fluid is transformed into elastic energy, part of which serves to deform the pipe (expansion) and the other to compress the fluid. When the wave reaches the reservoir, at $t = L/C_f$ the pressure is uniform, and all the fluid is under the extra head H and all the kinetic energy is transformed into elastic energy.

Event 2: To restore the equilibrium between the pressures of the reservoir and the pipe, the fluid flows backward at the same initial velocity since the pressure of the reservoir is constant. A low-pressure wave is superimposed to the existing

overpressure (Fig. **1.1b**). At $t = 2L/C_f$, the kinetic energy of the previous event stored in the form of elastic strain energy is restored. The pressure is back to normal along the pipe (to H_0) and the velocity is equal to V_0.

Event 3: The fluid continues to flow towards the reservoir and subsequently the pressure decreases at the valve by *H* meters lesser than H_0 . The low-pressure wave reflected by the closed valve travels back to the reservoir (Fig. **1.1c**). The pressure is set to $H_0 - H$ on the entire pipe at $t = 3L/C_f$. Then, the fluid is expanding while the pipe is contracting in latera direction.

Event 4: The unbalanced conditions at the reservoir cause the fluid to flow downstream at the velocity V_0 and a positive-pressure wave progresses forward to the valve. The pipe and the fluid return to normal conditions (Fig. **1.1d**). At the instant, the high-pressure wave reaches the valve, the fluid and pipe conditions are the same as $4L/C_f$ seconds earlier. This process is then repeated every period $T = 4L/C_f$.

Water hammer process can be visualized in the space-time plane as illustrated in Fig. (**1.2**). The sloped dashed lines represent the wave fronts corresponding to either high-pressure or low-pressure waves with increasing time. These lines divide the space-time plane into zones at different pressures and different velocities.

Noting that the analysis of water hammer process in case of a sudden stoppage of a pump, of a flow in a discharge pipe is the same except, however that it begins with a pressure drop and ends with an overpressure. It would be enough to repeat the explanations given above starting with event 3.

Pressure wave-speed

The pressure wave-speed depends on the physical properties of the fluid and the mechanical and geometrical characteristics of the pipe. Its determination requires the search for the celerity of the acoustic wave in the fluid in question. The starting formula concerns the blood flow in the vessels as $C_{f0} = \left(K/\rho_f\right)^{1/2}$ with *K* is the bulk modulus of the fluid.

CHAPTER 2

Mathematical Development

Abstract: This chapter gives a detailed description of the mathematical development proposed for the study. The elasticity theory and the general theory of beams are strongly present whereas some assumptions are adopted to simplify the analysis.

Keywords: Creep; Elastic pipelines; Fluid-structure interaction; Poisson coupling; Viscoelasticity.

INTRODUCTION

The mathematical development of the water hammer models is based on two equations : (i) the continuity equation and (ii) the momentum equation. Both of them represent an independent mechanical law. When applied to the fluid in the pipe, *e.g.*, water, the two equations lead to establishing the partial differential equation (PDE) of the fluid, which constitutes the classical water hammer model described in Chapter 1. However, if fluid structure interaction (FSI) is involved, then two other equations are added leading to the four-equation model. The procedure is applied to water hammer and cavitation in both elastic and viscoelastic pipelines.

WATER HAMMER IN ELASTIC PIPELINES

Introduction

Water hammer in elastic pipelines (metallic ad concrete pipelines) is considered in this section. The pipe of inner diameter D, thickness e and inclination γ contains a moving fluid. At each section of the pipe, one can define the steady state velocity V and the pressure p. The four-equation model (4EM) is used to determine these two variables for the fluid and the axial velocity and the axial stress for the pipe. The formulation of the 4EM is based on two basic principles: the continuity principle and the energy conservation principle. The FSI in liquid-filled piping systems is modelled by extended water hammer theory for the fluid and the Timoshenko beam theory and elasticity theory (Hooke's law) for the pipe [2, 45 and

69]. Thus, two governing equations for the fluid are coupled to two governing equations for the pipe by means of boundary conditions, representing the contact between the fluid and the pipe-wall at the interface.

Assumptions

Schwartz introduced the following assumptions in order to simplify the analysis [2 and 16]:

- Transient flow is one-dimensional: pressure *p* and velocity *V* are uniform on each section *A* of the pipeline.
- Convective terms are neglected since the velocity *V* is very smaller than the pressure wave celerity C_f. This assumption is called *acoustic approximation.*
- The pressure waves propagate at low frequencies in axial direction; radial inertia effect is neglected.
- The fluid is homogeneous, isotropic and has linearly elastic behavior.
- The material of the pipe is isotropic and homogeneous, and it has a quasi-rigid linear elastic behavior (metals and concrete).
- The pipe has a circular thin-walled section.
- Cavitation does not occur: the fluid pressure remains above the vapour pressure.

Fluid Dynamics

The cylindrical coordinate system is considered. For an infinitesimal fluid volume ϑ, the continuity equation can be derived in its local form [70]:

$$\frac{\partial \rho_f}{\partial t} + V_r \frac{\partial \rho_f}{\partial r} + \frac{V_\varphi}{r} \frac{\partial \rho_f}{\partial \varphi} + V_z \frac{\partial \rho_f}{\partial z} + \rho_f \, div\vec{V} = 0 \qquad \textbf{(2.1)}$$

The equation of state is:

$$\frac{\partial \rho_f}{\partial t} = \frac{\rho_f}{K} \frac{\partial p}{\partial t} \qquad \textbf{(2.2)}$$

in which *K* is the bulk modulus of compressibility of the fluid. Since the fluid is homogeneous, its density does not depend on space variables, *i.e.*, $\partial \rho_f / \partial r = \partial \rho_f / \partial z = \partial \rho_f / \partial \varphi = 0$. After neglecting the circumferential part of the velocity [2], Eqs. (2.1) and (2.2) lead to the continuity equation of the fluid.

$$\frac{1}{K}\frac{\partial p}{\partial t}+\frac{\partial V_z}{\partial z}+\frac{1}{r}\frac{\partial}{\partial r}\left(rV_r\right)=0 \qquad \textbf{(2.3)}$$

For the same infinitesimal volume ϑ, the equation of motion can also be written in a local form as:

$$\rho_f \frac{d\vec{V}}{dt}=-\overrightarrow{grad}\,p+\overrightarrow{div}\,\bar{\bar{\tau}}+\vec{F} \qquad \textbf{(2.4)}$$

with $\vec{F}$ is the outside force per unit volume and $\bar{\bar{\tau}}$ denotes the viscosity stress tensor given by:

$$\bar{\bar{\tau}}=\left(\mu'-\frac{2}{3}\mu\right)div\vec{V}\,\bar{\bar{I}}+2\mu\bar{\bar{D}} \qquad \textbf{(2.5)}$$

with μ and μ' are respectively dynamic and volumetric viscosity coefficients, $\bar{\bar{I}}$ is the identity matrix and $\bar{\bar{D}}$ is the strain tensor defined as:

$$\bar{\bar{D}}=\frac{1}{2}\left(\overline{\overline{grad}}\,\vec{V}+\left(\overline{\overline{grad}}\,\vec{V}\right)^t\right) \qquad \textbf{(2.6)}$$

Eqs. (2.5) and (2.6) can be introduced in Eq. (2.4) and lead to the Navier-Stokes equation.

$$\rho_f \frac{d\vec{V}}{dt}=\rho_f\vec{F}-\overrightarrow{grad}\,p+\mu\Delta\vec{V}+\left(\mu'+\frac{1}{3}\mu\right)\overrightarrow{grad}\left(div\vec{V}\right) \qquad \textbf{(2.7)}$$

in which the coefficient μ' is equal to zero. The left-hand side of Eq. (2.7) is a particular derivative that can be developed as:

$$\rho_f \frac{d\vec{V}}{dt}=\rho_f\left(\frac{\partial\vec{V}}{\partial t}+\left(\overline{\overline{grad}}\,\vec{V}\right)\vec{V}\right) \qquad \textbf{(2.8)}$$

in which:

CHAPTER 3

Numerical Calculation of Water Hammer

Abstract: In this chapter, the Method of Characteristics (MOC) is detailed and used to solve the mathematical models defined in the second chapter, where the reservoirpipe-valve-system is considered. The wave-speed adjustment (WSA) scheme is preferred for the MOC. The numerical method is applied to the elastic pipelines on onehand and to the viscoelastic pipelines on the other hand.

Keywords: Boundary conditions; Initial conditions; Linear interpolation; Method of characteristics; Wave-speed adjustment.

INTRODUCTION

The partial derivative equations (PDE) describe numerous physical phenomena such as wave propagation. They can be classified with respect to their order (usually 1st or 2nd order) and their coefficients (linear, quasi-linear or nonlinear). The unknowns usually depend on time t and space x or z. The PDE problems are successfully solved by means of the MOC. However, this method needs numerical schemes and computational grids. Since interpolation leads to numerical oscillations in the result. The WSA scheme is preferred and then applied to the water hammer models already developed, such as the four-equation friction model.

THE METHOD OF CHARACTERISTICS (MOC)

The conventional form of 1st linear PDE systems with constant coefficients is:

$$\mathbf{A}\frac{\partial \mathbf{y}}{\partial t} + \mathbf{B}\frac{\partial \mathbf{y}}{\partial z} = \mathbf{r} \qquad \textbf{(3.1)}$$

with **A** and **B** are two matrices, **y** is the vector of unknowns and **r** is the right-hand side vector.

Abdelaziz Ghodhbani, Ezzeddine Haj Taïeb, Mohsen Akrout & Sami Elaoud

Compatibility Equations

The characteristic equation of (3.1) is:

$$\det\left(\mathbf{B}-\lambda\mathbf{A}\right)=0 \tag{3.2}$$

Three situations are possible according to the roots of Eq. (3.2): (i) if all roots are reals number, the system 3.1 is hyperbolic; (ii) if all roots are reals and equal, the system is parabolic and (iii) if all roots are imaginary numbers, the system is elliptic.

The Method of Characteristics (MOC) is preferred for calculation of PDE systems. Eq. (3.1) is equivalent to [2]:

$$\frac{\partial\mathbf{y}}{\partial t}+\mathbf{A^{-1}B}\frac{\partial\mathbf{y}}{\partial z}=\mathbf{A^{-1}r} \tag{3.3}$$

According to linear algebra, it is known that for every square matrix with strict real elements, it exists a matrix **S** such that:

$$\mathbf{S^{-1}}\left(\mathbf{A^{-1}B}\right)\mathbf{S}=\mathbf{D} \tag{3.4}$$

in which the matrix **D** is diagonal and is written in case of four unknowns as

$$\mathbf{D}=\begin{bmatrix}\lambda_1 & 0 & 0 & 0\\ 0 & \lambda_2 & 0 & 0\\ 0 & 0 & \lambda_3 & 0\\ 0 & 0 & 0 & \lambda_4\end{bmatrix}$$

The eigenvalues λ_i are the characteristic directions. Their calculation can be obtained by solving the following equation:

$$\det\left(\mathbf{A^{-1}B}-\lambda\mathbf{I^4}\right)=0 \tag{3.5}$$

which is equivalent to:

$$\det\left[\mathbf{A}^{-1}\left(\mathbf{B}-\lambda\mathbf{A}\right)\right]=0 \tag{3.6}$$

To solve the above equation, one needs a regular matrix **T**:

$$\mathbf{T}=\mathbf{S}^{-1}\mathbf{A}^{-1} \tag{3.7}$$

which implies:

$$\mathbf{D}=\mathbf{TBS} \text{ and } \mathbf{TB}=\mathbf{DS}^{-1} \tag{3.8}$$

Eq. (3.7) leads to:

$$\mathbf{S}^{-1}=\mathbf{TA} \tag{3.9}$$

Hence, the introduction of Eq. (3.9) into Eq. (3.8) leads to:

$$\mathbf{TB}=\mathbf{DTA} \tag{3.10}$$

The multiplication of the system (3.1) by the matrix **T** and the consideration of Eq. (3.10) allows a new formulation of the system:

$$\mathbf{TA}\frac{\partial\mathbf{y}}{\partial t}+\mathbf{DTA}\frac{\partial\mathbf{y}}{\partial z}=\mathbf{Tr} \tag{3.11}$$

By considering the vector $\mathbf{v}=\mathbf{TAy}$, it follows:

$$\frac{\partial\mathbf{v}}{\partial t}+\mathbf{D}\frac{\partial\mathbf{v}}{\partial z}=\mathbf{Tr} \tag{3.12}$$

which is detailed in the following:

$$\frac{\partial v_i}{\partial t}+\lambda_i\frac{\partial v_i}{\partial z}=\left(Tr\right)_i \tag{3.13}$$

The differentiation of v_i gives:

$$\frac{dv_i}{dt}=\frac{\partial v_i}{\partial t}+\frac{dz}{dt}\frac{\partial v_i}{dz} \tag{3.14}$$

CHAPTER 4

Numerical Modelling of Transient Cavitation

Abstract: The modelling of transient cavitation is described in this chapter by considering column separation modelling where FSI and gas release are taken into account. As detailed for water hammer modelling, transient in straight pipeline is caused by fast closure of shut-off valve. Both vaporous and gaseous cavitation are considered in the numerical models.

Keywords: Cavity; Collapse; Column separation; Discrete model; Gas release; pressure pulse, Vaporous cavitation.

INTRODUCTION

Transient cavitation occurs in piping systems through two modes: liquid column separation and distributed cavitation. This latter is described in the literature through the bubble model, while the discrete vapour cavity model is widely used when column separation is assumed to occur, which is the case of the present study. In this study, the emphasis is placed on the effect of fluid-structure interaction (FSI) on the solution. In fact, the chapter focuses on the numerical modelling of cavitation by considering four-equation models.

COLUMN SEPARATION MODELLING IN ELASTIC PIPES

The Coupled DVCM

General Concept

The coupled DVCM was proposed [52] to take account of FSI in the vaporous cavitation modelling; the model ignore the gas release effect. Transient is caused by a fast valve closure. Initial velocity is assumed to be high, so that vaporous cavitation and column separation occur. Moreover, thermodynamic conditions characterizing the classical DVCM, such as cavity opening and collapse and the constant vapour pressure in the cavity, are still valid. As described for the classical DVCM, vapour cavities are concentrated at the grid points, whereas liquid is

overlying the reaches. Nevertheless, the isothermal process is no longer adopted; the cavitation process is assumed to be isentropic.

The coupled DVCM is obtained by incorporating the classical DVCM into the compatibility equations (3.39) and (3.40) deriving from the 4EFM. The MOC based on the WSA scheme is used to solve the proposed model. The space-time plan is divided into regular mesh with a space step Δz and a time step Δt. While $H > H_v - z\sin\gamma$ with γ is the inclination of the pipe, cavitation does not occur, and the water hammer model is used. Once the pressure p drops below the gauge vapour pressure p_v at the computation point P, the strong condition $H = H_v - z\sin\gamma$ is established. Four unknowns are then calculated at each time step Δt: the upstream discharge q_u^P, the downstream discharge q_d^P, the axial velocity of the pipe $\dot{u}_z^P$ and the axial stress σ_z^P.

The coupled DVCM was calculated in a "stress wave" grid used in a specific form yielding two different schemes [52]. The first one is a full-WSA scheme that allows calculations at all points of the RG as shown in Fig. (**4.1**). This scheme can be used whether the integers a and b characterizing the WSA method are odd or even. The second one called WSA-TLI scheme allows calculations with the WSA method only at the first SG, whereas TLI provides information at points of the second SG. This scheme is illustrated in Fig. (**4.1**), where the integers a and b are indicative for calculation only. If a single SG is used instead of the RG, then calculations based on the WSA method cannot be performed unless both integers a and b are odd. Since these latter are chosen either odd or even with respect to the characteristic direction ratio r, the single SG is not useful. Therefore, the WSA-TLI scheme is assumed to be a helpful alternative for the full-WSA because it allows calculation of the coupled DVCM in a SG using the WSA method.

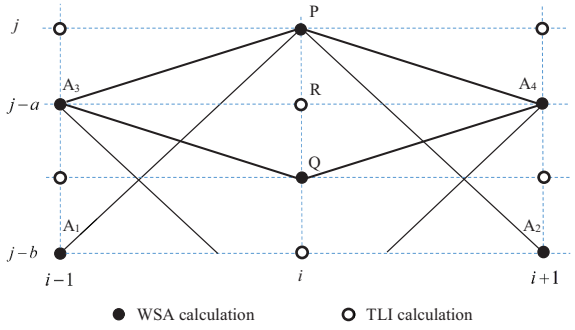

Fig. (4.1). "Stress wave" grid based on the WSA-TLI scheme [52].

The calculation of the hollow points shown in Fig. (**4.1**) using the TLI technique is simply obtained since the time step Δt is constant. For example, the discharge at the point R (earlier point of P) is:

$$q_u^R = \frac{1}{2}\left(q_u^Q + q_u^P\right) \text{ and } q_d^R = \frac{1}{2}\left(q_d^Q + q_d^P\right) \tag{4.1}$$

and so are $\dot{u}_z^R$ and σ_z^R. Then, the cavity volume $\forall_v$ is calculated at each point of the RG and the formula given by Eq. (1.19) is modified to:

$$\forall_v^P = \forall_v^Q + \Delta t\left[\psi\left(q_d^P - q_u^P\right) + (1-\psi)\left(q_d^Q - q_u^Q\right)\right] \tag{4.2}$$

Once the compatibility equations are integrated along the characteristic directions $+\tilde{C}_f$, $-\tilde{C}_f$ $+\tilde{C}_p$ and $-\tilde{C}_p$, the four governing equations of the vaporous cavitating flow are derived:

$$\frac{1}{A}\left(q_u^P - q_d^{A_1}\right) + K_f g\left(H^P - H^{A_1}\right) + \Sigma_f\left(\dot{u}_z^P - \dot{u}_z^{A_1}\right) - \frac{\Sigma_f}{\rho_p \tilde{C}_f}\left(\sigma_z^P - \sigma_z^{A_1}\right) = b\Delta t g\left[\left(\Gamma\Sigma_f - 1\right)h_{fd}^{A_1} + \Sigma_f \sin\gamma\right] \tag{4.3}$$

$$\frac{1}{A}\left(q_d^P - q_u^{A_2}\right) - K_f g\left(H^P - H^{A_2}\right) + \Sigma_f\left(\dot{u}_z^P - \dot{u}_z^{A_2}\right) + \frac{\Sigma_f}{\rho_p \tilde{C}_f}\left(\sigma_z^P - \sigma_z^{A_2}\right) = b\Delta t g\left[\left(\Gamma\Sigma_f - 1\right)h_{fu}^{A_2} + \Sigma_f \sin\gamma\right] \tag{4.4}$$

$$\frac{1}{A}\left(q_u^P - q_d^{A_3}\right) + K_p g\left(H^P - H^{A_3}\right) + \Pi\left(\dot{u}_z^P - \dot{u}_z^{A_3}\right) - \frac{\tilde{C}_p}{\Sigma_p E}\left(\sigma_z^P - \sigma_z^{A_3}\right) = a\Delta t g\left[\left(\Gamma\Pi - 1\right)h_{fd}^{A_3} + \Pi \sin\gamma\right] \tag{4.5}$$

CHAPTER 5

Numerical Results for Elastic Pipelines

Abstract: This chapter deals with the numerical results obtained from the simulation of fluid transients in elastic pipes. The MOC with WSA scheme is used and the numerical results are validated against experimental records. The comparison shows good agreement between the two results which validate the earlier proposed models.

Keywords: Experimental result; Fluid response; Poisson coupling; Structural response; Unsteady friction.

INTRODUCTION

Water hammer is simulated by use of the 4EM and the 4EFM with a comparison between the two models. In the former, Poisson coupling, and junction coupling can be revealed, while the latter takes account of the three dynamic coupling types. In addition, the unsteady friction (UF) effect is revealed by simulating the Zielke model as well as the Vardy-Brown model in both classical and coupled models. For cavitation, two coupled column separation models, namely the coupled DVCM and the coupled DGCM are proposed and compared against experimental results from the literature.

WATER HAMMER WITHOUT CAVITATION

It is worth noting that the negative values of pressure displayed in the following figures do not drop below -1.013 bar . The aim of this numerical simulation is to compare the WSA scheme to the linear interpolation schemes.

The Benchmark Problem A

The Benchmark Problem A (BPA) shown by Fig. (**5.1**) is used as numerical test and the exact solution of Tijsseling [2] is used to compare and evaluate the WSA scheme. Noting that the Delft Hydraulic Problems A to F have been defined and used to test numerical methods and FSI software. The BPA concerns a reservoir-pipe-valve system, where the straight steel-pipe is defined by its length $L = 20$ m , inner radius $R = 398.5$ mm , thickness $e = 8$ mm , Young's modulus $E = 210$ GPa ,

mass density $\rho_p = 8900$ kg.m^{-3} and Poisson coefficient $\nu = 0.30$. The water in the pipe has a bulk modulus of elasticity K = 2.1 GPa, mass density $\rho_f = 1000$ kg.m^{-3} and an initial velocity $V_0 = 1$ m.s^{-1}. The instantaneously closing valve may be fixed (no junction coupling) or free (with junction coupling). Tijsseling proposed and validated [80] the exact solution for the BPA against the MOC solution obtained with the WSA scheme proposed [81]. The calculation shown that the two solutions are almost identical.

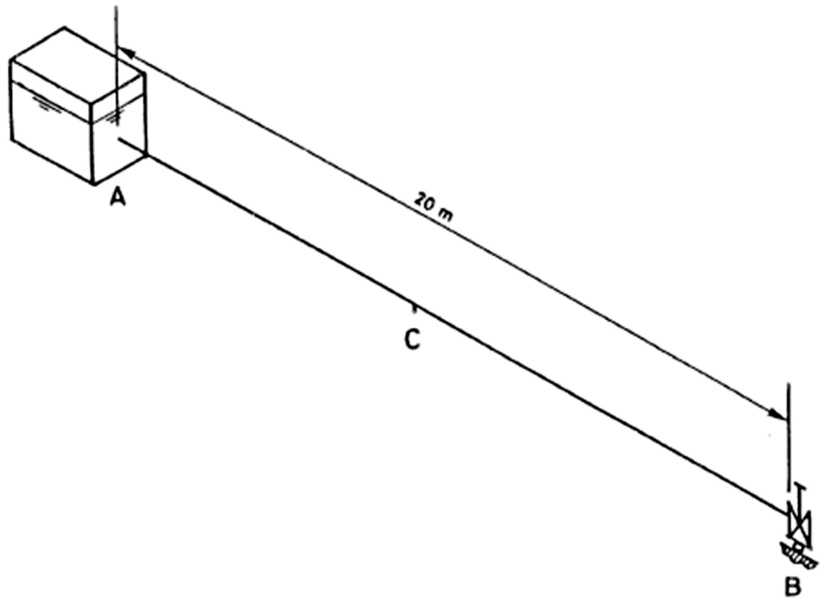

Fig. (5.1). Reservoir-pipe-valve system in Delft Hydraulics Benchmark Problem A [80].

Effect of Poisson Coupling

This subsection concerns the analysis of the Poisson coupling assumed to act without junction coupling: the valve is rigidly fixed to the support. The WSA scheme of the MOC is used to calculate the 4EM. The characteristic directions are $\tilde{C}_f = 1024{,}55$ m.s^{-1} and $\tilde{C}_p = 5280{,}5$ m.s^{-1} so that their ratio is $\tilde{C}_p / \tilde{C}_f = 5.1539$. Therefore, the integers $a = 13$ and $b = 67$ are chosen for the adjustment. Noting that the computations are obtained without any correction on the mass densities, because the result is practically not influenced with these

assumptions. Also, there is no discretization of the space domain; only one reach can be used, *i.e.* $N=1$ and $\Delta t=0.98$ ms. To calculate the pressure at the middle of the pipe, a minimum number of reaches $N=2$ will be sufficient. The effect of Poisson coupling on the pressure evolution at the valve is shown by Figs. (**5.2** and **5.3**). These figures also display the preference of the WSA scheme to both SLI and TLI schemes. The effect of the precursor wave on the pressure wave can be clearly observed. The precursor waves are pressure waves induced by the stress waves and propagate at the stress wave-speed C_p.

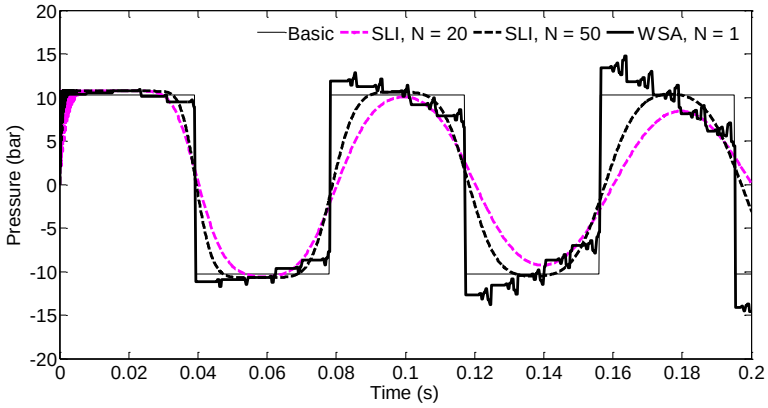

Fig. (5.2). Pressure at the fixed valve and preference of the WSA scheme to the SLI scheme in the BPA.

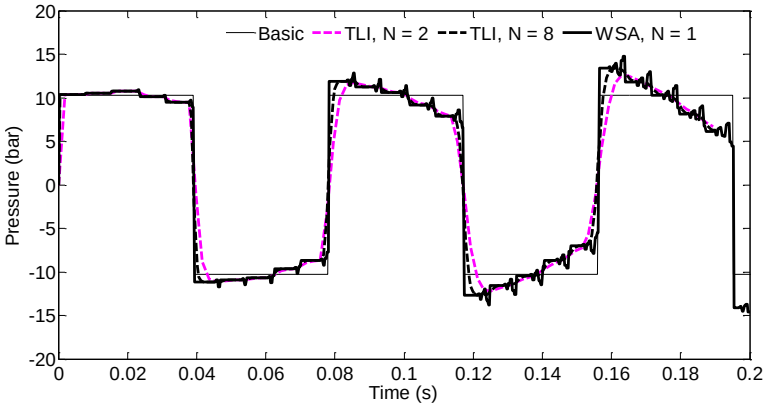

Fig. (5.3). Pressure at the fixed valve and preference of the WSA scheme to the TLI scheme in the BPA.

CHAPTER 6

Numerical Results for Viscoelastic Pipelines

Abstract: This chapter deals with the numerical results obtained from simulation of fluid transients in viscoelastic pipes. For the non-cavitating flow case, the simulation shows that the pressure fluctuations are rapidly attenuated, and the overall transient pressure wave is delayed in time due to the retarded deformation of the pipe-wall. In addition, the simulation of the cavitating flow gives reasonable results compared to experimental data.

Keywords: Circonferential strain; Creep-compliance; Experimental result; Viscoelastic pipelines.

INTRODUCTION

The viscoelastic behaviour of the polyethylene (PE) pipe determines the pressure response during transient. The calibrated creep functions provided by Covas in [1] are used in simulation of water hammer without cavitation. The experimental data of Stoinov and Covas are used to validate calculations of the classical models as well as the proposed models without cavitation.

Case Studies

Case 1: Water Hammer in HDPE Pipeline

The experiment of Stoinov and Covas carried out in 277 m HDPE pipeline, 63 mm diameter, at Imperial College (IC) is mainly used to validate numerical calculations. The experimental facility is presented in Subsection 6.4 of Chapter 1. The pipeline was fixed to a concrete structure with plastic brackets, 1 m spaced, and with metal frames at the elbows, to avoid any axial movement. This facility was particularly designed and constructed for the investigation of novel leak detection techniques based on the generation of transient events in a water pipe system. Collected transient data were essentially used for calibration and validation of the Hydraulic Transient Solver (HTS) and Inverse Transient Analysis (ITA) proposed by Covas in [1].

Transient pressure and circumferential strain data were collected at several sites. The effect of pipe-wall viscoelasticity was observed in specific features of the

Abdelaziz Ghodhbani, Ezzeddine Haj Taïeb, Mohsen Akrout & Sami Elaoud

transient pressure signal (*i.e.*, initial pressure peak and major energy dissipation) and in stress-strain curves during the occurrence of transient events (*i.e.* mechanical hysteresis). Viscoelastic behaviour is typically described by a creep-compliance function, $J(t)$. Results of the experimental tests were discussed, and final remarks were made on how to characterise the viscoelastic behaviour of PE as a material and when it is integrated in a water pipe system.

In 2003, Covas gave an extensive work in which she analysed the effects of several parameters on fluid and pipe responses: steady friction (SF), unsteady friction (UF), boundary conditions and viscoelasticity [1]. The emphasis was made on the major effect of viscoelastic behaviour on pressure and strain damping and dispersion. To obtain accurate results, calibrations of the transient solver was used. However, in the present study, any of these calibrations will be adopted; some relevant parameters mentioned in [1] will be useful, such as the ignorance of the UF effect (frictionless modelling), the number of Kelvin-Voight elements and the pressure wave-speed. Covas has calibrated her solver by carrying out a sensitivity analysis to define model parameters. Afterwards, calibrations were carried out for several transient tests considering laminar and smooth turbulent flow: $Q_0 = 0.056\ \text{l.s}^{-1}$ to $1.98\ \text{l.s}^{-1}$. The wave-speed is $C_f = 385\ \text{m.s}^{-1}$ to $425\ \text{m.s}^{-1}$ according to the estimated values based on maximum pressure peaks and travelling wave times. The elastic wave speed was fixed at $395\ \text{m.s}^{-1}$ (*i.e.* $E_0 = 1.4\ \text{GPa}$ and $J_0 = 0.70\ \text{GPa}^{-1}$) as a compromise between accuracy and computational time, and the relaxation times are equal to 0.05, 0.5, 1.5, 5 and 10 s. The best-fitted parameters, and the respective creep curves and calculated piezometric heads were detailed. It was concluded that the minimum number of three elements is essential to achieve an acceptable level of accuracy, and greater numbers (4 ou 5) do not improve the accuracy of the results, providing only a different combination of parameters J_k and requiring more computational time. In addition, the relaxation times $\tau_1 = 0.05\ \text{s}$ and $\tau_2 = 0.5\ \text{s}$ must be included in the K-V model to achieve a good accuracy of the model, and any of the others higher than the previous ones (*e.g.* $\tau_3 = 1.5\ \text{s}$, 5 s or 10 s) can be used. According to the tests of Stoinov and Covas, it has been assumed that the higher the relaxation times are, the closer calibrated creeps are to the experimental function. The analysis of sample size ΔT was carried out to determine the best relaxation time τ_3, and it was concluded that

creep functions for $\tau_3 = 10$ s are closer to the experimental curve than that for $\tau_3 = 1.5$ s and $\tau_3 = 5$ s.

Table **6.1** displays two series of viscoelastic parameters provided in [1] corresponding to two different cases used in this section to validate the numerical computation: the steady state laminar flow case $Q_0 = 0.056$ l.s^{-1} ($\mathrm{Re} = 1400$) and the steady state turbulent flow case $Q_0 = 1.008$ l.s^{-1} ($\mathrm{Re} = 25200$).

Table 6.1. Creep compliance functions for two cases of steady state flowrate.

Steady State Flowrate Q_0 (l/s)	**Sample SizΔ ΔT (s)**	**Average Least Square Error (m^2)**	**Creep Function J_k (10^{-9} Pa^{-1})**		
			τ_1 = 0.5 s	**τ_3 = 1.5 s**	**τ_3 = 10 s**
0.054	10	0.0014	0.0935	0.13	0.836
1.008	10	0.0472	0.104	0.124	0.41

The friction coupling is considered through steady friction (SF) terms expressed by the Darcy-Weisbach formula. The friction coefficient f can be obtained by the Blasius formula for turbulent flow and the Hagen-Poiseuille formula for laminar flow. Covas provided useful relationship between pipe friction and Reynolds number (Fig. **6.1**) [1]. According to this result, the friction coefficients used in this case study will be almost equal to 0.040 for the laminar flow and 0.025 for the smooth turbulent flow.

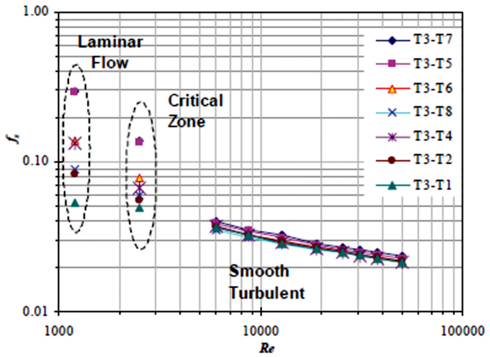

Fig. (6.1). Relationship between pipe friction and Reynolds number [1].

REVIEW AND CONCLUSIONS

In this work, fluid-structure interaction (FSI) modelling and numerical simulation of transient in pipelines have been carried out. The emphasis was made on the development of column separation models taking into account several parameters such as friction, Poisson coupling, junction coupling (axial movement of the pipe) and viscoelasticity. The derived equations are valid for long wavelength and hence low frequency. All mathematical and numerical modelling are based on the standard reservoir-pipe-valve system, where transient is caused by the fast closing of the downstream valve, except in case of cavitation in viscoelastic pipelines for which transient is caused by the quick closure of the upstream valve.

An extensive review of literature has been carried out. It has given description of physical phenomenon and mathematical and numerical modelling of hydraulic transients in pipelines. Several experiments on water hammer and cavitation in elastic and viscoelastic pipelines have been investigated. The proposed models of water hammer in pipelines have been developed based on the continuity equation and the momentum equation for both the fluid and the pipe. The modelling takes account of elasticity, unsteady friction, and viscoelasticity. Thus, three coupled models have been detailed allowing calculation of the pressure and the axial velocity of the fluid and the axial stress and the axial velocity of the pipe. These coupled models are in fact FSI models that take into account three types of dynamic coupling: friction coupling, Poisson coupling and junction coupling. The four-equation model (4EM) and the four-equation friction model (4EFM) describe water hammer in elastic pipes with free axial vibration. The numerical modelling of cavitation has been based on the water hammer models and the classical column separation models, namely the classical discrete vapour cavity model (DVCM) and the classical discrete gas cavity model DGCM. Both vaporous and gaseous cavitation have been studied by considering only column separation at specific locations along the pipeline. Distributed cavitation models have not been studied in this work.

Regarding the numerical procedure, the MOC has been used to solve the water hammer models in both elastic and viscoelastic models. The WSA scheme has been preferred to both time-line interpolation (TLI) and space-line interpolation (SLI) schemes. The MOC development based on the WSA scheme had been first applied

to the water hammer elastic models (the 4EM and the 4EFM) and then extended to cavitation.

The cavitation study has only considered column separation phenomenon, which is dominant in hydraulic plants. The cavitation modelling has been obtained by referring to the water hammer models. The compatibility equations of the water hammer models have been used to develop the coupled DVCM and the coupled DGCM for elastic pipelines. Therefore, the same approach has been extended to the viscoelastic pipelines. The MOC development has been also used to solve the coupled viscoelastic model referred to as the 4EVEM. This latter has needed further development because of the existence of the retarded strain in the governing equations. As proposed for the elastic pipelines, the compatibility equations of this model leaded to the coupled viscoelastic DVCM, referred to as coupled VE-DVCM. Moreover, gas release phenomenon was taken into account by providing the coupled DGCM which was only applied for elastic pipes.

The valve anchoring conditions were also considered in the coupled numerical models. For each model, the boundary condition at the valve was considered in two different modes. The first one corresponds to the fixed valve which ignores junction coupling. The second which is more complicated in calculation corresponds to the freely moving valve. This latter supposes that the valve can move axially so that the material of the support (whether rigid or viscoelastic) matters.

The developed models have been implemented in software package using computer codes developed by the present authors. The implementation of the numerical models into the software package using matrix transformation is detailed in appendix D where only the downstream-valve system is considered. The simulation and the manual calibration lead to the following conclusions:

i) The instantaneous closure valve is a successful way to cause transient; the discrepancy that it exhibits is negligible compared to the non-instantaneous closure valve, which causes nonlinearity and needs numerical method to solve.
ii) The WSA scheme is more reliable and more suitable than the interpolation schemes although some manual calibration are needed during calculation, and in addition, the density adjustment are not necessary, and they do not influence the result.
iii) The classical models of water hammer are as accurate as junction coupling is reduced. The rigid the pipe anchor is, the efficient the classical model is.

iv) The weakness of the classical column separation models (the DVCM and the DGCM) is their dependence to the mesh refinement and their non-convergence. Also, these models cannot predict structural responses.

v) The FSI models such as the four-equation model (4EM), the four-equation friction model (4EFM), the coupled DVCM and the coupled DGCM are preferred to the classical models regarding accuracy, convergence and computational efficiency. The 4EM 4EFM are preferred especially in case of axially vibrating pipes with quasi-rigid or viscoelastic supports.

vi) The main advantage of the FSI models is their ability to predict structural responses such as axial displacement, axial strain, and axial stress. The structural responses can be assumed to be accurate once the pressure history is validated against experimental results.

vii) In case of cavitation in elastic pipelines, the FSI models provide more accuracy even when the pipe is rigidly anchored. The coupled DVCM and the coupled DGCM proposed in this work have been validated in case of hydraulic system with fixed valve, but the proposed approach is also valid for freely moving pipes.

viii) The simulation shows that the support material has an important impact on fluid and structural responses during fluid transients in elastic pipelines, but the numerical simulation has not been validated with experimental results.

ix) Unsteady friction (UF) is more suitable because it yields more damping and more accuracy in elastic pipes. In viscoelastic pipes, its damping effect is negligible compared to the viscoelastic damping, and the calculation can be limited to the steady-state friction.

x) Gas release leads to more accuracy when considered whatever the model and whatever the pipe material (classical DGCM and coupled DGCM for elastic pipes and VE-DGCM for VE pipes).

xi) The classical viscoelastic models (VEM) for water hammer and cavitation can provide accurate results in case of anchored pipeline, and on would not need coupled models for this case, such as the 4EVEM and the coupled VE-DVCM, which can be more suitable in case of vibrating structures.

xii) Some structural responses such as the circumferential strain and the hoop stress can be accurately predicted with the classical VEM in case of rigidly anchored pipes.

xiii) Cavitation prediction in VE pipelines can be improved if the variable creep-compliance (VCC) approach is used instead of the constant creep-compliance (CCC) approach. The main advantage of the former consists in pressure magnitudes.

The modelling and the numerical simulation proposed for water hammer and cavitation in pipelines are analysed and detailed taking the most hydraulic and mechanical cases that can be observed in practice. Nonetheless, the study has not considered turbomachines (pumps and turbines) which represent important components in hydraulic plants and pipeline systems. The developed models have been validated against experimental results in case of valve-closure induced transients. Pump and turbine stopping, and failure and other events can be mathematically modelled and incorporated into the above models to predict fluid transients.

Appendices

Appendix A: Generalized Hook's Law

The generalized Hook's law is attributed to Robert Hooke who established in 1678 that the deformation of a structure is proportional to the applied forces. This law is valid for solid material with linear elastic behaviour. For one-dimensional configuration, the Hook's law is written by the linear relationship $\sigma = E\varepsilon$, in which avec σ is the strength stress, ε is the strain and E is the Young's modulus of elasticity.

In the three-dimensional system, σ and ε are no longer scalars but they are 2nd order tensors. The generalized Hook's law is defined in the cylindrical coordinate system as:

$$\begin{bmatrix} \sigma_r \\ \sigma_\varphi \\ \sigma_z \\ \tau_{r\varphi} \\ \tau_{\varphi z} \\ \tau_{zr} \end{bmatrix} = \begin{bmatrix} C_{11} & C_{12} & . & . & . & C_{16} \\ C_{21} & . & . & . & . & . \\ . & . & . & . & . & . \\ . & . & . & . & . & . \\ . & . & . & . & . & . \\ C_{61} & . & . & . & . & C_{66} \end{bmatrix} \begin{bmatrix} \varepsilon_r \\ \varepsilon_\varphi \\ \varepsilon_z \\ 2\varepsilon_{r\varphi} \\ 2\varepsilon_{\varphi z} \\ 2\varepsilon_{zr} \end{bmatrix} \quad \textbf{(A.1)}$$

which can be expressed as:

$$\sigma_{ij} = C_{ijkl}\varepsilon_{kl} \quad \textbf{(A.2)}$$

with **C** is the 4th order tensor of stiffness. Since $\boldsymbol{\sigma_{ij}}$ and $\boldsymbol{\varepsilon_{kl}}$ are symmetric, the components $\mathbf{C_{ijkl}}$ are reduced to 36. For homogeneous isotropic materials, the generalized Hook's law is:

$$\sigma_{ij} = \lambda \varepsilon_{kk} \delta_{ij} + 2\mu \varepsilon_{ij} \tag{A.3}$$

with λ denotes the Lamé coefficient, μ is the stiffness modulus, ε_{kk} is the trace of the matrix $\boldsymbol{\varepsilon_{kl}}$ given by $\varepsilon_{kk} = \varepsilon_r + \varepsilon_\varphi + \varepsilon_z$, and δ_{ij} is the Kronecker's index. The development of Eq. (A.3) leads to:

$$\begin{aligned}
\sigma_{ij} &= \lambda \varepsilon_{kk} \delta_{ij} + 2\mu \varepsilon_{ij} \\
\sigma_r &= \lambda \varepsilon_{kk} + 2\mu \varepsilon_r \\
\sigma_\varphi &= \lambda \varepsilon_{kk} + 2\mu \varepsilon_\varphi \\
\sigma_z &= \lambda \varepsilon_{kk} + 2\mu \varepsilon_z \\
\tau_{r\varphi} &= 2\mu \varepsilon_{r\varphi} \\
\tau_{\varphi z} &= 2\mu \varepsilon_{\varphi z} \\
\tau_{zr} &= 2\mu \varepsilon_{zr}
\end{aligned} \tag{A.4}$$

It follows:

$$\sigma_{kk} = \left(3\lambda + 2\mu\right) \varepsilon_{kk} \tag{A.5}$$

The incorporation of Eq. (A.5) into Eq. (A.3) allows:

$$\varepsilon_{ij} = \frac{1}{2\mu}\left(\sigma_{ij} - \frac{\lambda}{3\lambda + 2\mu} \sigma_{kk} \delta_{ij} \right) \tag{A.6}$$

which is usually written as:

$$\varepsilon_{ij} = \frac{1+\nu}{E} \sigma_{ij} - \frac{\nu}{E} \sigma_{kk} \delta_{ij} \tag{A.7}$$

With E is the Young's modulus of elasticity given by $E = \mu(3\lambda + 2\mu)/(\lambda + \mu)$ and ν is the Poisson's coefficient defined by $\nu = \lambda/[2(\lambda + \mu)]$. In the cylindrical coordinate system, Eq. (A.7) is:

$$\varepsilon_r = \frac{\partial u_r}{\partial r} = \frac{1}{E}\left[\sigma_r - \nu\left(\sigma_\varphi + \sigma_z\right)\right] \quad \textbf{(A.8)}$$

$$\varepsilon_\varphi = \frac{u_r}{r} = \frac{1}{E}\left[\sigma_\varphi - \nu\left(\sigma_r + \sigma_z\right)\right] \quad \textbf{(A.9)}$$

$$\varepsilon_z = \frac{\partial u_z}{\partial z} = \frac{1}{E}\left[\sigma_z - \nu\left(\sigma_r + \sigma_\varphi\right)\right] \quad \textbf{(A.10)}$$

$$\varepsilon_{r\varphi} = \frac{1+\nu}{E}\tau_{r\varphi} \quad \textbf{(A.11)}$$

$$\varepsilon_{\varphi z} = \frac{1+\nu}{E}\tau_{\varphi z} \quad \textbf{(A.12)}$$

$$\varepsilon_{zr} = \frac{1+\nu}{E}\tau_{zr} \quad \textbf{(A.13)}$$

The above equations lead to:

$$\sigma_r = \frac{E}{(1+\nu)(1-2\nu)}\left[(1-\nu)\varepsilon_r + \nu\left(\varepsilon_\varphi + \varepsilon_z\right)\right] \quad \textbf{(A.14)}$$

$$\sigma_\varphi = \frac{E}{(1+\nu)(1-2\nu)}\left[(1-\nu)\varepsilon_\varphi + \nu\left(\varepsilon_r + \varepsilon_z\right)\right] \quad \textbf{(A.15)}$$

$$\sigma_z = \frac{E}{(1+\nu)(1-2\nu)}\left[(1-\nu)\varepsilon_z + \nu\left(\varepsilon_r + \varepsilon_\varphi\right)\right] \quad \textbf{(A.16)}$$

and subsequently,

$$\sigma_r = E\varepsilon_r + \nu\left(\sigma_\varphi + \sigma_z\right) \quad \textbf{(A.17)}$$

$$\sigma_{\varphi} = \frac{E}{1-\nu^2}\left(\varepsilon_{\varphi} + \nu\varepsilon_z\right) + \frac{\nu}{1-\nu}\sigma_r \qquad \textbf{(A.18)}$$

$$\sigma_z = \frac{E}{1-\nu^2}\left(\varepsilon_z + \nu\varepsilon_{\varphi}\right) + \frac{\nu}{1-\nu}\sigma_r \qquad \textbf{(A.19)}$$

Appendix B: Stress Distribution in a Pressurized Ring

In this appendix, a circular section pipe of inner radius R and wall thickness e is considered. A constant pressure p is maintained inside the pipe while the pressure p_{out} (like the barometric pressure) is assumed to exist outside. In order to express radial and hoop stress in the pipe, a thin ring is considered (Fig. **B.1**). The bi-harmonic Airy's function Φ can be used in polar coordinate system. By neglecting the inertial effect of both the fluid and the pipe, the Airy's function satisfies:

$$\Delta^4 \Phi = 0 \qquad \textbf{(B.1)}$$

In addition, if the Airy's function is independent of the angle φ, then the development of Eq. B.1 gives:

$$\frac{d^4\Phi}{dr^4} + \frac{2}{r}\frac{d^3\Phi}{dr^3} - \frac{1}{r^2}\frac{d^2\Phi}{dr^2} + \frac{1}{r^3}\frac{d\Phi}{dr} = 0 \qquad \textbf{(B.2)}$$

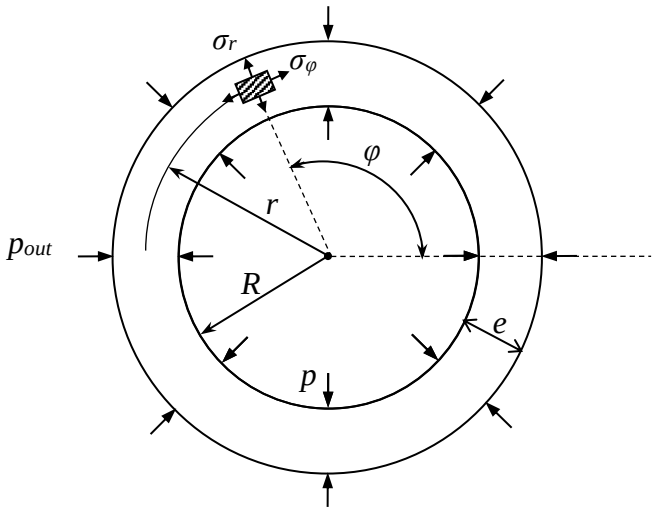

Fig. (B.1). Stress distribution in pressurized ring.

By taking $r = \exp(t)$, the general solution for the above differential equation is:

$$\phi = A\,\mathrm{Log}\,r + Br^2\,\mathrm{Log}\,r + Cr^2 + D \qquad \textbf{(B.3)}$$

Moreover, if the volume densities of forces are neglected, the stresses are:

$$\sigma_r = \frac{1}{r^2}\frac{\partial^2\phi}{\partial r^2} + \frac{1}{r}\frac{\partial\phi}{\partial r} \qquad \textbf{(B.4)}$$

$$\sigma_\varphi = \frac{\partial^2\phi}{\partial r^2} \qquad \textbf{(B.5)}$$

Thus, by taking account of Eq. (B.3), it follows:

$$\sigma_r = \frac{A}{r^2} + B(1 + 2\log r) + 2C \qquad \textbf{(B.6)}$$

$$\sigma_\varphi = -\frac{A}{r^2} + B(3 + 2\log r) + 2C \qquad \textbf{(B.7)}$$

$$\tau_{r\varphi} = 0 \qquad \textbf{(B.8)}$$

The condition $B = 0$ resulting from the displacement condition leads to:

$$\sigma_r = \frac{A}{r^2} + 2C \qquad \textbf{(B.9)}$$

$$\sigma_\varphi = -\frac{A}{r^2} + 2C \qquad \textbf{(B.10)}$$

The constants of integration are obtained thanks to the boundary conditions $(\sigma_r)_{r=R} = -p$ and $(\sigma_r)_{r=R+e} = -p_{out}$, hence:

$$\frac{A}{R^2} + 2C = -p \qquad \textbf{(B.11)}$$

$$\frac{A}{(R+e)^2} + 2C = -p_{out} \tag{B.12}$$

which implies:

$$A = \frac{R^2 (R+e)^2}{2\left(R+\frac{1}{2}e\right)e}(p_{out} - p) \tag{B.13}$$

$$2C = \frac{R^2 p - (R+e)^2 p_{out}}{2\left(R+\frac{1}{2}e\right)e} A \tag{B.14}$$

Consequently,

$$\sigma_r = \frac{1}{(2R+e)e}\left[-R^2\left(\frac{(R+e)^2}{r^2} - 1\right)p + (R+e)^2\left(\frac{R^2}{r^2} - 1\right)p_{out} \right] \tag{B.15}$$

$$\sigma_\varphi = \frac{1}{(2R+e)e}\left[R^2\left(\frac{(R+e)^2}{r^2} + 1\right)p - (R+e)^2\left(\frac{R^2}{r^2} + 1\right)p_{out} \right] \tag{B.16}$$

In case of $p_{out} = 0$, Eqs. (B.15) and (B.16) become:

$$\sigma_r = \frac{R^2}{(2R+e)e}\left(1 - \frac{(R+e)^2}{r^2}\right)p \tag{B.17}$$

$$\sigma_\varphi = \frac{R^2}{(2R+e)e}\left(1 + \frac{(R+e)^2}{r^2}\right)p \tag{B.18}$$

Eqs. (B.17) and (B.18) show that σ_r is a compression stress and σ_φ is a strength stress that takes its maximum at the outside surface of the pipe:

$$\sigma_{\varphi.\max} = \frac{2R^2}{(2R+e)e}\, p \qquad \textbf{(B.19)}$$

Appendix C: Calculation of the Classical Water Hammer Model Using the MOC

The standard reservoir-pipe-valve system is considered. Water hammer is caused by the fast valve closure. The integration of the compatibility equations (1.) leads to:

$$C_f{}^{+}:\ H\Big|_i^j - H\Big|_{i-1}^{j-1} + \frac{C_f}{g}\left(V\Big|_i^j - V\Big|_{i-1}^{j-1}\right) + \frac{f\Delta z}{2gD} V\Big|_{i-1}^{j-1}\Big|V\Big|_{i-1}^{j-1}\Big| = 0 \qquad \textbf{(C.1)}$$

$$C_f{}^{-}:\ H\Big|_i^j - H\Big|_{i+1}^{j-1} - \frac{C_f}{g}\left(V\Big|_i^j - V\Big|_{i+1}^{j-1}\right) - \frac{f\Delta z}{2gD} V\Big|_{i+1}^{j-1}\Big|V\Big|_{i+1}^{j-1}\Big| = 0 \qquad \textbf{(C.2)}$$

Eq. (C.1) is valid for $dz/dt = +C_f$, whereas Eq. (C.2) is valid for $dz/dt = -C_f$. It follows:

$$H\Big|_i^j = \frac{1}{2}\left[H\Big|_{i-1}^{j-1} + H\Big|_{i+1}^{j-1} + \frac{C_f}{g}\left(V\Big|_{i-1}^{j-1} - V\Big|_{i+1}^{j-1}\right)\right] - \frac{f\Delta z}{4gD}\left(V\Big|_{i-1}^{j-1}\Big|V\Big|_{i-1}^{j-1}\Big| - V\Big|_{i+1}^{j-1}\Big|V\Big|_{i+1}^{j-1}\Big|\right) \qquad \textbf{(C.3)}$$

$$V\Big|_i^j = \frac{1}{2}\left[V\Big|_{i-1}^{j-1} + V\Big|_{i+1}^{j-1} + \frac{g}{C_f}\left(H\Big|_{i-1}^{j-1} - H\Big|_{i+1}^{j-1}\right)\right] - \frac{f\Delta t}{4D}\left(V\Big|_{i-1}^{j-1}\Big|V\Big|_{i-1}^{j-1}\Big| + V\Big|_{i+1}^{j-1}\Big|V\Big|_{i+1}^{j-1}\Big|\right) \qquad \textbf{(C.4)}$$

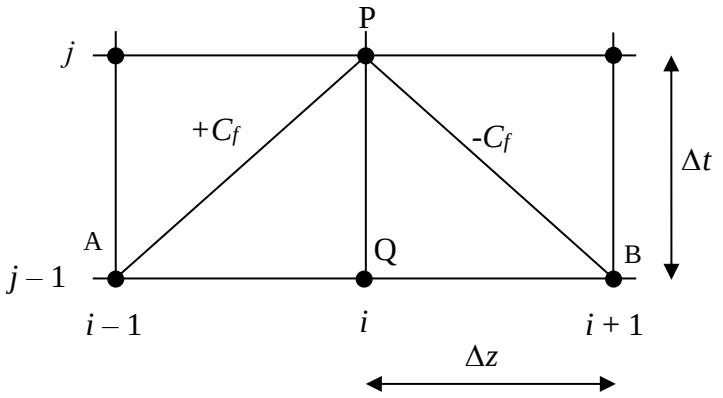

Fig. (C.1). Characteristic directions in the (z, t) plan.

Initial conditions are the steady state conditions characterized by the fluid velocity which is assumed to be uniform at each section and the pressure head given, thanks to the Darcy-Weisbach formula:

$$H_0(z) = H_{res} - \frac{fV_0^2}{2gD} z \qquad \textbf{(C.5)}$$

with H_{res} is the constant head of the reservoir.

Boundary conditions are derived from the physical properties of the hydraulic configuration. One equation is needed at each end of the pipe. At the upstream end (constant head reservoir), one can write:

$$H\Big|_1^j = H_{res} \qquad \textbf{(C.6)}$$

And at the downstream end (instantaneous closure valve):

$$V\Big|_{N+1}^j = 0 \qquad \textbf{(C.7)}$$

Appendix D: Algebraic System Components for Calculation of the FSI Models

To facilitate the computer programme implementation of the FSI model (four-equation model), the numerical integration of the compatibility equations can be written in general form as follows [89]:

$$\mathbf{My = k + diag}\left(\mathbf{MY}\right) \tag{D.1}$$

with **M** is the coefficient matrix, **y** is the vector of unknowns, **Y** is the matrix of calculated variables and **k** is the first right-hand side vector; the second right-hand side vector is the diagonal of the matrix **MY**. Table **D.1** illustrates these mathematical items for each FSI model.

Table D.1. Algebraic system components for FSI models [89].

FSI model	Coefficient matrix			Vector y	Matrix Y	Right hand side vector		
	Inner sections	Reservoir	valve (fixed/free)			Inner sections	Reservoir	valve (fixed/free)
4EM and 4EFM	**M1**	**R1**	**V1**	**y1**	**Y1**	**k1**	**r1**	**v1**
Coupled DVCM	**M2**	**R2**	**V2**	**y2**	**Y2**	**k2**	**r2**	**v2**
Coupled DGCM	**M2**	**R2**	**V2**	**y2**	**Y2**	**k2**	**r2**	**v2**
4EVEM	**M3**	**R3**	**V3**	**y1**	**Y1**	**k3**	**r3**	**v3**
Coupled VEDVCM	**M4**	**R4**	**V4**	**y2**	**Y2**	**k4**	**r4**	**v4**

In the following expressions:

- The superscript Q denotes the one-step earlier point from the computational point P.
- For the column separation models, the piezometric head at the computational point P is $H^P = H_v - z\sin\gamma$.

It is worth noting that the expressions of matrices and vectors at boundaries are only valid for the downstream valve system; the calculation of the upstream valve system (case of cavitation in VE pipelines in this work) can be obtained similarly according to its boundary conditions.

It is also noted that some expressions used at boundary conditions such as $\hat{\gamma}_1$ and $\hat{\gamma}_2$ in the vector **r4** should be calculated separately.

Coefficient Matrices

$$\mathbf{M1}=\begin{bmatrix} 1 & K_f g & \Sigma_f & -\dfrac{\Sigma_f}{\rho_p \tilde{C}_f} \\ 1 & -K_f g & \Sigma_f & \dfrac{\Sigma_f}{\rho_p \tilde{C}_f} \\ 1 & K_p g & \Pi & -\dfrac{\tilde{C}_p}{\Sigma_p E} \\ 1 & -K_p g & \Pi & \dfrac{\tilde{C}_p}{\Sigma_p E} \end{bmatrix};\mathbf{M2}=\begin{bmatrix} 1/A & 0 & \Sigma_f & -\dfrac{\Sigma_f}{\rho_p \tilde{C}_f} \\ 0 & 1/A & \Sigma_f & \dfrac{\Sigma_f}{\rho_p \tilde{C}_f} \\ 1/A & 0 & \Pi & -\dfrac{\tilde{C}_p}{\Sigma_p E} \\ 0 & 1/A & \Pi & \dfrac{\tilde{C}_p}{\Sigma_p E} \end{bmatrix}$$

$$\mathbf{M3}=\begin{bmatrix} 1 & K_f g - b\hat{C}_1 \dfrac{D}{2e}\rho_f g J & \Sigma_f & -\dfrac{\Sigma_f}{\rho_p \tilde{C}_f} \\ 1 & -K_f g + b\hat{C}_1 \dfrac{D}{2e}\rho_f g J & \Sigma_f & \dfrac{\Sigma_f}{\rho_p \tilde{C}_f} \\ 1 & K_p g - a\hat{C}_2 \dfrac{D}{2e}\rho_f g J & \Pi & -\dfrac{\tilde{C}_p}{\Sigma_p E} \\ 1 & -K_p g + a\hat{C}_2 \dfrac{D}{2e}\rho_f g J & \Pi & \dfrac{\tilde{C}_p}{\Sigma_p E} \end{bmatrix};\mathbf{M4}=\begin{bmatrix} 1/A & 0 & \Sigma_f & -\dfrac{\Sigma_f}{\rho_p \tilde{C}_f} \\ 0 & 1/A & \Sigma_f & \dfrac{\Sigma_f}{\rho_p \tilde{C}_f} \\ 1/A & 0 & \Pi & -\dfrac{\tilde{C}_p}{\Sigma_p E} \\ 0 & 1/A & \Pi & \dfrac{\tilde{C}_p}{\Sigma_p E} \end{bmatrix}$$

$$\mathbf{R1}=\begin{bmatrix} 0 & 1 & 0 & 0 \\ 1 & -K_f g & \Sigma_f & \dfrac{\Sigma_f}{\rho_p \tilde{C}_f} \\ 0 & 0 & 1 & 0 \\ 1 & -K_p g & \Pi & \dfrac{\tilde{C}_p}{\Sigma_p E} \end{bmatrix};\ \mathbf{R2}=\begin{bmatrix} 1 & -1 & 0 & 0 \\ 0 & 1/A & \Sigma_f & \dfrac{\Sigma_f}{\rho_p \tilde{C}_f} \\ 0 & 0 & 1 & 0 \\ 0 & 1/A & \Pi & \dfrac{\tilde{C}_p}{\Sigma_p E} \end{bmatrix}$$

$$\mathbf{R3}=\begin{bmatrix} 0 & 1 & 0 & 0 \\ 1 & -K_f g + b\hat{C}_1 \dfrac{D}{2e}\rho_f g J & \Sigma_f & \dfrac{\Sigma_f}{\rho_p \tilde{C}_f} \\ 0 & 0 & 1 & 0 \\ 1 & -K_p g + a\hat{C}_2 \dfrac{D}{2e}\rho_f g J & \Pi & \dfrac{\tilde{C}_p}{\Sigma_p E} \end{bmatrix};\mathbf{R4}=\begin{bmatrix} 1 & -1 & 0 & 0 \\ 0 & 1/A & \Sigma_f & \dfrac{\Sigma_f}{\rho_p \tilde{C}_f} \\ 0 & 0 & 1 & 0 \\ 0 & 1/A & \Pi & \dfrac{\tilde{C}_p}{\Sigma_p E} \end{bmatrix}$$

For fixed valve:

$$\mathbf{V1}=\begin{bmatrix} 1 & K_f g & \Sigma_f & -\dfrac{\Sigma_f}{\rho_p \tilde{C}_f} \\ 1 & 0 & 0 & 0 \\ 1 & K_p g & \Pi & -\dfrac{\tilde{C}_p}{\Sigma_p E} \\ 0 & 0 & 1 & 0 \end{bmatrix};\ \mathbf{V2}=\begin{bmatrix} 1/A & 0 & \Sigma_f & -\dfrac{\Sigma_f}{\rho_p \tilde{C}_f} \\ 0 & 1 & 0 & 0 \\ 1/A & 0 & \Pi & -\dfrac{\tilde{C}_p}{\Sigma_p E} \\ 0 & 0 & 1 & 0 \end{bmatrix}$$

$$\mathbf{V3}=\begin{bmatrix} 1 & K_f g-b\hat{C}_1\dfrac{D}{2e}\rho_f gJ & \Sigma_f & -\dfrac{\Sigma_f}{\rho_p\tilde{C}_f} \\ 1 & 0 & 0 & 0 \\ 1 & K_p g-a\hat{C}_2\dfrac{D}{2e}\rho_f gJ & \Pi & -\dfrac{\tilde{C}_p}{\Sigma_p E} \\ 0 & 0 & 1 & 0 \end{bmatrix};\ \mathbf{V4}=\begin{bmatrix} 1/A & 0 & \Sigma_f & -\dfrac{\Sigma_f}{\rho_p\tilde{C}_f} \\ 0 & 1 & 0 & 0 \\ 1/A & 0 & \Pi & -\dfrac{\tilde{C}_p}{\Sigma_p E} \\ 0 & 0 & 1 & 0 \end{bmatrix}$$

For free valve:

$$\mathbf{V1}=\begin{bmatrix} 1 & K_f g & \Sigma_f & -\dfrac{\Sigma_f}{\rho_p\tilde{C}_f} \\ 1 & 0 & -1 & 0 \\ 1 & K_p g & \Pi & -\dfrac{\tilde{C}_p}{\Sigma_p E} \\ 0 & -A\rho_f g & \dfrac{m}{\Delta t}+c+\dfrac{k\Delta t}{2} & A_p \end{bmatrix};\ \mathbf{V2}=\begin{bmatrix} 1/A & 0 & \Sigma_f & -\dfrac{\Sigma_f}{\rho_p\tilde{C}_f} \\ 0 & 1 & -1 & 0 \\ 1/A & 0 & \Pi & -\dfrac{\tilde{C}_p}{\Sigma_p E} \\ 0 & 0 & \dfrac{m}{\Delta t}+c+\dfrac{k\Delta t}{2} & A_p \end{bmatrix}$$

$$\mathbf{V3}=\begin{bmatrix} 1 & K_f g-b\hat{C}_1\dfrac{D}{2e}\rho_f gJ & \Sigma_f & -\dfrac{\Sigma_f}{\rho_p\tilde{C}_f} \\ 1 & 0 & 0 & 0 \\ 1 & K_p g-a\hat{C}_2\dfrac{D}{2e}\rho_f gJ & \Pi & -\dfrac{\tilde{C}_p}{\Sigma_p E} \\ 0 & -A\rho_f g & \dfrac{m}{\Delta t}+c+\dfrac{k\Delta t}{2} & A_p \end{bmatrix};\ \mathbf{V4}=\begin{bmatrix} 1/A & 0 & \Sigma_f & -\dfrac{\Sigma_f}{\rho_p\tilde{C}_f} \\ 0 & 1 & -1 & 0 \\ 1/A & 0 & \Pi & -\dfrac{\tilde{C}_p}{\Sigma_p E} \\ 0 & 0 & \dfrac{m}{\Delta t}+c+\dfrac{k\Delta t}{2} & A_p \end{bmatrix}$$

Matrices of Calculated Variables

$$\mathbf{Y1}=\begin{bmatrix} V_z^{A_1} & V_z^{A_2} & V_z^{A_3} & V_z^{A_4} \\ H^{A_1} & H^{A_2} & H^{A_3} & H^{A_4} \\ \dot{u}_z^{A_1} & \dot{u}_z^{A_2} & \dot{u}_z^{A_3} & \dot{u}_z^{A_4} \\ \sigma_z^{A_1} & \sigma_z^{A_2} & \sigma_z^{A_3} & \sigma_z^{A_4} \end{bmatrix};\ \mathbf{Y2}=\begin{bmatrix} Q_u^{A_1} & Q_u^{A_2} & Q_u^{A_3} & Q_u^{A_4} \\ Q_d^{A_1} & Q_d^{A_2} & Q_d^{A_3} & Q_d^{A_4} \\ \dot{u}_z^{A_1} & \dot{u}_z^{A_2} & \dot{u}_z^{A_3} & \dot{u}_z^{A_4} \\ \sigma_z^{A_1} & \sigma_z^{A_2} & \sigma_z^{A_3} & \sigma_z^{A_4} \end{bmatrix}$$

Vectors of Unknowns

$$\mathbf{y1}=\begin{bmatrix} V_z \\ H \\ \dot{u}_z \\ \sigma_z \end{bmatrix};\quad \mathbf{y2}=\begin{bmatrix} Q_u \\ Q_d \\ \dot{u}_z \\ \sigma_z \end{bmatrix}$$

First Right-hand Side Vectors

$$\mathbf{k1}=\begin{bmatrix} b\Delta tg\left[\left(\Gamma\Sigma_f-1\right)h_f^{A_1}+\Sigma_f\sin\gamma\right] \\ b\Delta tg\left[\left(\Gamma\Sigma_f-1\right)h_f^{A_2}+\Sigma_f\sin\gamma\right] \\ a\Delta tg\left[\left(\Gamma\Pi-1\right)h_f^{A_3}+\Pi\sin\gamma\right] \\ a\Delta tg\left[\left(\Gamma\Pi-1\right)h_f^{A_4}+\Pi\sin\gamma\right] \end{bmatrix};\ \mathbf{k2}=\mathbf{k1}+\begin{bmatrix} -K_f g\left(H^P-H^{A_1}\right) \\ K_f g\left(H^P-H^{A_2}\right) \\ -K_p g\left(H^P-H^{A_3}\right) \\ K_p g\left(H^P-H^{A_4}\right) \end{bmatrix};$$

$$\mathbf{k3} = \mathbf{k1} + \begin{bmatrix} b\Delta t\hat{\gamma}_1 \\ -b\Delta t\hat{\gamma}_1 \\ a\Delta t\hat{\gamma}_2 \\ -a\Delta t\hat{\gamma}_2 \end{bmatrix}; \ \mathbf{k4} = \mathbf{k1} + \begin{bmatrix} b\Delta t\hat{\gamma}_1 - K_f g\left(H^P - H^{A_1}\right) + b\Delta t\hat{C}_1 \dfrac{\partial\left(\varepsilon_{\varphi r}\right)^P}{\partial t} \\ -b\Delta t\hat{\gamma}_1 + K_f g\left(H^P - H^{A_2}\right) - b\Delta t\hat{C}_1 \dfrac{\partial\left(\varepsilon_{\varphi r}\right)^P}{\partial t} \\ a\Delta t\hat{\gamma}_2 - K_p g\left(H^P - H^{A_3}\right) + a\Delta t\hat{C}_2 \dfrac{\partial\left(\varepsilon_{\varphi r}\right)^P}{\partial t} \\ -a\Delta t\hat{\gamma}_2 + K_p g\left(H^P - H^{A_4}\right) - a\Delta t\hat{C}_2 \dfrac{\partial\left(\varepsilon_{\varphi r}\right)^P}{\partial t} \end{bmatrix}$$

$$\mathbf{r1} = \begin{bmatrix} H_{res} \\ b\Delta tg\left[\left(\Gamma\Sigma_f - 1\right)h_f^{A_2} + \Sigma_f \sin\gamma\right] \\ 0 \\ a\Delta tg\left[\left(\Gamma\Pi - 1\right)h_f^{A_4} + \Pi\sin\gamma\right] \end{bmatrix}; \ \mathbf{r2} = \mathbf{r1} + \begin{bmatrix} 0 \\ K_f g\left(H^P - H^{A_2}\right) \\ 0 \\ K_p g\left(H^P - H^{A_4}\right) \end{bmatrix}$$

$$\mathbf{r3} = \mathbf{r1} + \begin{bmatrix} 0 \\ -b\Delta t\hat{\gamma}_1 \\ 0 \\ -a\Delta t\hat{\gamma}_2 \end{bmatrix}; \ \mathbf{r4} = \mathbf{r1} + \begin{bmatrix} 0 \\ -b\Delta t\hat{\gamma}_1 + K_f g\left(H^P - H^{A_2}\right) - b\Delta t\hat{C}_1 \dfrac{\partial\left(\varepsilon_{\varphi r}\right)^P}{\partial t} \\ 0 \\ -a\Delta t\hat{\gamma}_2 + K_p g\left(H^P - H^{A_4}\right) - a\Delta t\hat{C}_2 \dfrac{\partial\left(\varepsilon_{\varphi r}\right)^P}{\partial t} \end{bmatrix}$$

For fixed valve:

$$\mathbf{v1}=\begin{bmatrix} b\Delta tg\left[\left(\Gamma\Sigma_f-1\right)h_f^{A_1}+\Sigma_f\sin\gamma\right] \\ 0 \\ a\Delta tg\left[\left(\Gamma\Pi-1\right)h_f^{A_3}+\Pi\sin\gamma\right] \\ 0 \end{bmatrix};\ \mathbf{v2}=\mathbf{v1}+\begin{bmatrix} -K_f g\left(H^P-H^{A_1}\right) \\ 0 \\ -K_p g\left(H^P-H^{A_3}\right) \\ 0 \end{bmatrix}$$

$$\mathbf{v3}=\mathbf{v1}+\begin{bmatrix} b\Delta t\hat{\gamma}_1 \\ 0 \\ a\Delta t\hat{\gamma}_2 \\ 0 \end{bmatrix};\quad \mathbf{v4}=\mathbf{v1}+\begin{bmatrix} b\Delta t\hat{\gamma}_1-K_f g\left(H^P-H^{A_1}\right)+b\Delta t\hat{C}_1\dfrac{\partial\left(\varepsilon_{\varphi r}\right)^P}{\partial t} \\ 0 \\ a\Delta t\hat{\gamma}_2-K_p g\left(H^P-H^{A_3}\right)+a\Delta t\hat{C}_2\dfrac{\partial\left(\varepsilon_{\varphi r}\right)^P}{\partial t} \\ 0 \end{bmatrix}$$

For free valve:

$$\mathbf{v1}=\begin{bmatrix} b\Delta tg\left[\left(\Gamma\Sigma_f-1\right)h_f^{A_1}+\Sigma_f\sin\gamma\right] \\ 0 \\ a\Delta tg\left[\left(\Gamma\Pi-1\right)h_f^{A_3}+\Pi\sin\gamma\right] \\ \left(\dfrac{m}{\Delta t}-\dfrac{k\Delta t}{2}\right)\dot{u}_z^Q-ku_z^Q+A\rho_f gL\sin\gamma \end{bmatrix};\ \mathbf{v2}=\mathbf{v1}+\begin{bmatrix} -K_f g\left(H^P-H^{A_1}\right) \\ 0 \\ -K_p g\left(H^P-H^{A_3}\right) \\ 0 \end{bmatrix}$$

$$\mathbf{v3} = \mathbf{v1} + \begin{bmatrix} b\Delta t\hat{\gamma}_1 \\ 0 \\ a\Delta t\hat{\gamma}_2 \\ 0 \end{bmatrix};$$

Appendix E: Frequency Dependent Friction

The unsteady friction approach consists in incorporating an additional term into the momentum equation in order to further consideration of the frictional and the inertial effects of the non-uniform velocity profile. The slope of the energy line h_f is decomposed respectively into two terms: steady-state term and unsteady term.

$$h_f = h_{f.s} + h_{f.u} \tag{E.1}$$

Unsteady friction models derive from the extra losses caused by the two-dimensional nature of the unsteady velocity profile [90]. Several types of unsteady friction models exist in the literature and are described in [91]. By assuming the velocity V is uniform on each section A, Zielke defined the head loss h_f as a sum of a steady-state part defined by the Darcy-Weisbach formulae and an unsteady part [90].

$$h_f = \frac{f}{2gD} V|V| + \frac{16\nu'}{gD^2}\left(\frac{\partial V}{\partial t} * W\right)(t) \tag{E.2}$$

where W is the weighting function, in time, ν' is the kinematic viscosity and (*) denotes convolution. The unsteady term follows from the convolution of the weighting function W with past temporal velocity variations.

$$\left(\frac{\partial V}{\partial t} * W\right)(t) = \int_0^t \frac{\partial V}{\partial t}(u) \cdot W(t-u)\, du \tag{E.3}$$

The convolution-based unsteady frictional head loss term in a staggered grid (SG), called *full convolution scheme* is [92]:

$$h_f(z,t) = \frac{fV(z,t)\left|V(z,t)\right|}{2gD} + \frac{16\nu'}{gD^2}\sum_{j=1,3,5,\ldots}^{M}\left[V(z,t-j\Delta t+\Delta t)-V(z,t-j\Delta t-\Delta t)\right]W(j\Delta t) \quad \textbf{(E.4)}$$

With $M = t/\Delta t - 1$. The weighting functions are defined in terms of the dimensionless time $\tau = 4\nu' t/D^2$ [92]. For laminar flow, Zielke has developed the weighting functions by assuming a constant kinematic viscosity [53, 59, 89,90-92]. For turbulent flow, the Vardy-Brown's model is obtained by deriving weighting functions for smooth pipes and rough pipes by using a linearly varied frozen turbulent viscosity in the shear-layer and infinite viscosity in the core [92].

$$W(\tau) = \frac{A^* \exp\left(-B^*\tau\right)}{\sqrt{\tau}} \quad \textbf{(E.5)}$$

with A^* and B^* are fitted coefficients to a more complex theoretical weighting function. For smooth pipes, the coefficients are:

$$A^* = \frac{1}{2}\sqrt{\frac{\nu'_w}{\pi\nu'_{lam}}}, \quad B^* = \frac{\mathrm{Re}^{\kappa}}{12.86} \quad \text{and} \quad \kappa = \log\left(15.29\,\mathrm{Re}^{-0.0567}\right) \quad \textbf{(E.6)}$$

where ν'_{lam} is the laminar kinematic viscosity and ν'_w is the kinematic viscosity at the pipe wall. For fully rough-pipe turbulent flow, the Vardy-Brown's coefficients become:

$$A^* = 0.0103\sqrt{\mathrm{Re}}\left(\frac{\varepsilon}{D}\right)^{0.39} \quad \text{and} \quad B^* = 0.0352\,\mathrm{Re}\left(\frac{\varepsilon}{D}\right)^{0.41} \quad \textbf{(E.7)}$$

in which, the relative roughness ε/D is in the range from 10^{-6} to 10^{-2}.

BIBLIOGRAPHY

[1] D.I.C. Covas, "Inverse transient analysis for leak detection and calibration of water pipe systems modelling special dynamic effects", In: PhD Thesis, Department of Civil and Environmental Engineering, Imperial College of Science, Technology and Medecine. London, UK, 2003.
[2] A.S. Tijsseling, "Fluid structure interaction in case of waterhammer with cavitation", In: Ph.D. Thesis, Delft University of Technology, Faculty of Civil Engineering, Communication on Hydraulic and Geotechnical Engineering. Delft, Netherlands, 1993, pp. 93-96.
[3] L-F. Ménabréa, "Note on the effect of water impact on pipes", Compte Rendus Hebdomadaires des Sciences de l'Académie des Sciences, Paris, France, vol. I, pp. 221-224, 1958.
[4] L-F. Ménabréa, "Note on the effect of water impact on pipes", Annals of Civil Engineering, Paris, France, vol. I, pp. 269-275, 1962.
[5] N. Joukowsky, "Hydraulic water hammer in water filled pipelines", In: Memory of the Scientific Imperial Academy of St-Petersbourg., vol. 9. Germany, 1900.
[6] E.B. Wylie, and V.L. Streeter, Fluid transients. McGraw-Hill: New York, USA, 1993.
[7] W. Weber, "Wave propagation theory in water or other incompressible liquid in elastic pipes", Mathematical-Physical Section, Leipzig, Germany, vol. 18, pp. 353-357, 1866.
[8] A.I. Moens, The Pulsation. E.J. Brill. Leydn, Hollande, 1878.
[9] D.J. Korteweg, "Sound speed in elastic pipes", Annals of Physics and Chemestry, vol. 5, no. 12, pp. 542-525, 1878.
[10] J. Parmakian, Waterhammer analysis. Prentice-Hall: New York, US, 1955.
[11] V.L. Streeter, and E.B. Wylie, Hydraulic transients. McGraw-Hill: New York, USA, 1967.
[12] I.S. Gromeka, "On the velocity of propagation of wave-like motion of fluids in elastic tubes". Physical-Mathematical Section of the Scientific Society of the Imperial University of Kazan: Kazan, Russia, 1883, pp. 1-19. (in Russian)
[13] H. Lamb, "On the velocity of sound in a tube, as affected by the elasticity of the walls", Memoirs of the Manchester Literary and Philosophical Society, vol. 42, Manchester, UK, pp. 1-16, 1898.
[14] R. Skalak, "An extended of the theory of waterhammer", Trans of the ASME, vol. 78, no. 1, pp. 105-116, 1956.
[15] A.R.D. Thorley, "Pressure transients in hydraulic pipelines", *J. Basic Eng*., vol. 91, no. 3, pp. 453-460, 1969.
[http://dx.doi.org/10.1115/1.3571152]
[16] A.S. Tijsseling, A.E. Vardy, and D. Fan, "Fluid-structure interaction and cavitation in a single-elbow pipe system", *J. Fluids Struct*., vol. 10, no. 4, pp. 395-420, 1996.
http://dx.doi.org/10.1006/jfls.1996.0025
[17] A.G.T.J Heinsbroek, "Fluid-structure interaction in non-rigid pipeline systems, Nuclear Engineering and Design", Delft Hydraulics, no. 172, pp. 123-135, 1997.
[18] G.B. Wallis, "One-dimensional two-phase flow". McGraw-Hill: New York, US, 1969.
[19] F.R. Young, Cavitation. McGraw-Hill: London, UK, 1989.
[20] E. Haj Taïeb, "Transient flow in deformable pipes with vapour cavitation and dissolved air release", In: Thesis report, Faculty of Sciences of Tunis. Tunisia, 1999.

[21] F. Caupin, and E. Herbert, "Cavitation in water: A review", laboratory of statistic physics of the higher normal school. French: Paris, pp. 1000-1017, 2006.
[22] A.Bergant, A. Tijsseling, J. Vitkovsky, and A. Simpson, "Discrete vapour cavity model with improved timing of opening and collapse of cavities", Proc. 2nd IAHR International Meeting of the Workgroup on Cavitation and Dynamic Problems in Hydraulic Machinery and Systems, Timişoara, Romania pp. 117-128, 2007.
[23] A.R.D. Thorley, "Fluid transients in pipeline systems", In: Thermo-Fluids Engineering Research Center, 1st City University: London EC1V 0HB, UK, 1991.
[24] A.R. Simpson, "Large water hammer pressures due to column separation in sloping pipes", In: Thermo-Fluids Engineering Research Center, 1st City University: London EC1V 0HB, UK, 1986.
[25] A. Bergant, J. Vitkovsky, A. Simpson, M. Lambert, and A. Tijsseling, "Discrete vapour cavity model with efficient and accurate unsteady friction term", Department of mathematics and computer science, Yokohama, Japan, 2006.
[26] T.H. Hogg, and J.J. Trail, "Discussion of Speed changes of hydraulic turbine for sudden changes of load by E.B. Strowger & S.L. Kerr"., Trans. Of the ASME, vol. 48, pp. 252-257, 1926.
[27] A. Langevin, "Bulletin of the technical building union", *France*, 1928.
[28] J.N. LeConte, "Experiments and calculations on the resurge phase of water hammer", *Trans. Am. Soc. Mech. Eng*., vol. 59, no. 8, pp. 691-694, 1937. [http://dx.doi.org/10.1115/1.4020577]
[29] H.R. Lupton, "Graphical analysis of pressure surges in piping systems", Trans of the ASME, vol. 59, pp. 691-694, 1953.
[30] I.C. O'Neill, "Water-hammer in simple pipe systems", In: MSc Thesis, University of Melbourne. Melbourne, Australia, 1959.
[31] B.B. Sharp, "Cavity formation in simple pipes due to rupture of water column", Nature, vol. 185, no. 4709, pp. 302-303, 1960. [http://dx.doi.org/10.1038/185302b0]
[32] B.B. Sharp, "The growth and collapse of cavities produced by a rarefaction wave with particular reference to rupture of water column", In: PhD. Thesis, The university of Melbourne. Melbourne, Australia, 1965.
[33] B.B. Sharp, "Rupture of water column", Proceeding of the 2nd Australasian Conf. on Hydraulics and Fluid Mechanics, Auckland, New Zealand pp. A169-A176, 1965.
[34] V. Jordan, "The Influence of check valves on water hammer at pump failure", Strojniski Vestnik, vol. 7, no. 4, 5, pp. 19-21, 1961.
[35] A.R. Simpson, and E.B. Wylie, "Towards an improved understanding of waterhammer column separation in pipelines,Civil Engineering Transactions 1989", Institution of Engineers, Australia, vol. CE31, no. 3, pp. 113-120, 1989.
[36] J.J. Shu, "Modelling vaporous cavitation on fluid transients", international journal of pressure vessels and piping, school of mechanical and production engineering, nanyang technological university, 50 nanyang avenue., no. 80, pp. 187-195, 2003.
[37] F. Knapp, "Discussion of experiments and calculations on the resurge phase of water hammer", Transactions of the ASME 61, pp. 440-441, 1939.
[38] V. Jordan, "Prediction of water hammer at pump failure without surge protection under water column separation conditions", In: PhD Thesis, University of Belgrade. Belgrade, Yugoslavia, 1965.
[39] G. Pezzinga, and D. Cannizzaro, "Analysis of transient vaporous cavitation in pipes by a distributed 2D model", J. Hydraul. Eng., vol. 140, no. 6, p. 04014019, 2014.

[http://dx.doi.org/10.1061/(ASCE)HY.1943-7900.0000840]

[40] W. Zielke, and H.D. Perko, "Low-pressure phenomena and water hammer analysis", 3R international, vol. 24, pp. 348-355, 1985.

[41] S.W. Kieffer, "Sound speeds in liquid-gas mixtures: Water-air and water-steam", JGR, vol. 182, no. 20, pp. 2895-2904, 1977.
[http://dx.doi.org/10.1029/JB082i020p02895]

[42] R.W. Angus, "Water hammer in pipes, including those supplied by centrifugal pumps: Graphical treatment", *Proc.- Inst. Mech. Eng*., vol. 136, no. 1, pp. 245-331, 1937.
[http://dx.doi.org/10.1243/PIME_PROC_1937_136_021_02]

[43] A.Bergant, Transient cavitating flow in pipelines. PhD Thesis, University of Ljubljana: Ljubljana, Slovenia, 1992.

[44] A.E. Vardy, and D. Fan, "Flexural waves in a closed tube", Proc. of the 5th Int. Conf. on Pressure Surges, pp. 43-47, 1989.

[45] D.H. Wilkinson, and E.M. Curtis, "Waterhammer in a thin-walled pipe", Proc. of the 3rd Int. Conf. on Pressure Surges, pp. 221-2240, 1980.

[46] A.S. Tijsseling, "Skalak's extended theory of water hammer", In: Journal of Sound and Vibration, Department of Mathematics and Computer Science. University of Technology of Eindhoven: Eindhoven, The Netherlands, no. 310, pp. 718-728, 2007.

[47] L. Hadj-Taïeb, "Vapour cavitation in transient flow with fluid-structure interaction", In: Thesis report. National Engineering School of Sfax: Sfax, Tunisia, 2008.

[48] B.B. Sharp, "A simple model for water column rupture", In: Proceeding of the 17th IAHR Congress, Baden-Baden, Germany no. 5, pp. 155-161, 1977.

[49] A.S. Tijsseling, and C.S.W. Lavooij, "Waterhammer with fluid-structure interaction", *Appl. Sci. Res*., vol. 47, no. 3, pp. 273-285, 1990.
[http://dx.doi.org/10.1007/BF00418055]

[50] D. Fan, and A. Tijsseling, "Fluid-structure interaction with cavitation in transient pipe flows", *Fluids Eng*., vol. 114, no. 2, pp. 268-274, 1992.
[http://dx.doi.org/10.1115/1.2910026]

[51] A.S. Tijsseling, "Fluid structure interaction in liquid-filled pipe systems: A review", *J. Fluids Struct*., vol. 10, no. 2, pp. 109-146, 1996.
[http://dx.doi.org/10.1006/jfls.1996.0009]

[52] A.Ghodhbani, M. Akrout, and E. Haj Taïeb, "Coupled approach and calculation of the discrete vapour cavity model", In: Journal of Fluids and Structures. Department of Civil Engineering, University of Dundee: Dundee, UK, no. 10, pp. 109-146, 2019.
[http://dx.doi.org/10.1016/j.jfluidstructs.2019.102691]

[53] A.Bergant, and A.R. Simpson, "Estimating unsteady friction in transient cavitating pipe flow", 2nd International Conference on Water Pipeline Systems, Edinburg, Scotland pp. 3-15, 1994.

[54] V.O.P. Ostrada, "Investigation on the effects of entrained air in pipelines". Dissertation, University of Stuttgart, Heft 158: Stuttgart, Germany, 2007.

[55] A.H. De Vries, Cavitation due to waterhammer in horizontal pipelines with several high points. Delft, The Netherlands, 1973.Delft Hydraulics Laboratory, Report M 1152. Delft, The Netherlands, 1973.

[56] G.A. Provoost, "Investigation into cavitation in a prototype pipeline caused by water hammer", Proc. of the Second International Conference on Pressure Surges, pp. 13-29, 1976.

[57] G.A. Provoost, and E.B. Wylie, "Discrete gas model to represent distributed free gas in liquids", In: Proceedings of the 5th International Symposium on Water Column Separation, IAHR, Obernach, Germany. Also: Delft Hydraulics Laboratory, Publication No. 263, 1982.

[58] E.B. Wylie, "Simulation of vaporous and gaseous cavitation", *J. Fluids Eng*., vol. 106, no. 3, pp. 307-311, 1984.
[http://dx.doi.org/10.1115/1.3243120]

[59] A.Ghodhbani, and E. Haj Taïeb, "A four-equation friction model for water hammer calculation in quasi-rigid pipelines", In: Int. Journal of Pressure Vessels and Piping, Department of Mechanical Engineering, National Engineering School of Sfax: Sfax, Tunisia, pp. 54-62, 2017.

[60] J.P.T. Kalkwijk, and C. Kranenburg, "Cavitation in horizontal pipelines due to water hammer", *J. Hydraul. Div*., vol. 97, no. 10, pp. 1585-1605, 1971.
[http://dx.doi.org/10.1061/JYCEAJ.0003106]

[61] J.P.T. Kalkwijk, and C. Kranenburg, "Closure to cavitation in horizontal pipelines due to water hammer", *J. Hydraul. Div*., vol. 99, no. 3, pp. 529-530, 1973.
[http://dx.doi.org/10.1061/JYCEAJ.0003599]

[62] C. Kranenburg, "Gas release during transient cavitation in pipes", *J. Hydra. Div*., vol. 100, no. 10, 1974.
[http://dx.doi.org/10.1061/JYCEAJ.0004077]

[63] C. Kranenburg, "Transient cavitation in pipelines", PhD Thesis, Delft University of Technology, Dept. of Civil Engineering, Laboratory of Fluid Mechanics, Delft, The Netherlands. Also: Communications on Hydraulics Delft University of Technology, Dept. of Civil Engineering, Report No. 73-2, 1973, 1974.

[64] C. Kranenburg, "The effect of free gas on cavitation in pipelines induced by water hammer", In: Proceedings of the First International Conference on Pressure Surges, pp. 41-52, 1972.

[65] L. Haj-Taïeb, and E. Hadj-Taïeb, "Effect of pipe-wall viscoelasticity on vapour cavitation in transient flow", In: J. Theoretical and Applied mechanics. National Engineering School of Sfax: Sfax, Tunisia, 2007.

[66] A.Bergant, and A.R. Simpson, "Water hammer and column separation measurements in an experimental apparatus". Dept. of Civil and Environmental Engineering: University of Adelaide, Adelaide, Australia, 1995.

[67] D.I.C Covas, "The dynamic effect of pipe wall viscoelasticity in hydraulic transients. Part I-experimental analysis and creep characterization", In: Department of Civil and Environmental Engineering, Imperial College of Science, Technology and Medecine. London, UK, 2004.

[68] A.K. Soares, D.I.C. Covas, H.M. Ramos, and L.F.R. Reis, "Unsteady flow with cavitation in viscoelastic pipes", *Int. J. Fluid Mach. Syst*., vol. 2, no. 4, pp. 269-277, 2009.
[http://dx.doi.org/10.5293/IJFMS.2009.2.4.269]

[69] C.S.W. Lavooij, and A.S. Tusseling, "Fluid-structure interaction in liquid-filled piping systems", *J. Fluids Struct*., vol. 5, no. 5, pp. 573-595, 1991.
[http://dx.doi.org/10.1016/S0889-9746(05)80006-4]

[70] J. Coirier, Continuum mechanics., 2nd Ed. Higher National School of Mechanics and Aerautechnics (ENSMA) of Poitier: Paris, French, 2001.

[71] A.Keramat, A. Tijsseling, Q. Hou, and A. Ahmadi, "Fluid-structure interaction with pipe-line viscoelasticity during water hammer", In: Journal of Fluids and Structures. Department of Civil Engineering, University of Technology of Shahrood: Shahrood, Iran, 2012, no. 28, pp. 434-455.

[72] R. Zanganeh, A. Ahmadi, and A. Keramat, "Fluid-structure interaction with viscoelastic supports during waterhammer in pipelines", Journal of Fluids and Structures, vol. 54, Department of Civil Engineering, University of Technology of Shahrood: Shahrood, Iran, pp. 215-311, 2014.

[73] D.I.C. Covas, I. Soianov, J.F. Mano, H. Ramos, and N. Graham, The dynamic effect of pipe wall viscoelasticity in hydraulic transients. Part I-model development, calibration and

verification. Department of Civil and Environmental Engineering, Imperial College of Science, Technology and Medecine: London, UK, 2005.
[http://dx.doi.org/10.1080/00221680509500111]

[74] S. Henclik, Analytical solution and numerical study on water hammer in a pipeline closed with an elastically attached valve. Journal of sound and vibration, Department of Hydropower, Institute of Fluid-flow Machinery, Polish Academy of Sciences: Gdansk, Poland, 417 (2018), pp. 245-259, 2018.
[http://dx.doi.org/10.1016/j.jsv.2017.12.011]

[75] A.Ghodhbani, E. Haj Taïeb, and M. Akrout, "Effect of anchor conditions on structural responses during fluid transients in pipelines", Proceedings of the Seventh International Conference on Advances in Mechanical Engineering and Mechanics (ICAMEM), Hammamet, Tunisia 2019.

[76] D.D. Budney, D.C. Wiggert, and F.J. Hatfield, "The influence of structural damping on internal pressure during a transient pipe flow", Transactions of the ASME, *J. Fluids Eng*., vol 113, pp. 424-429, 1991.
[http://dx.doi.org/10.1115/1.2909513]

[77] A.Bergant, and A.S. Tijsseling, Parameters affecting water hammer wave attenuation, shape and timing. Litostroj E.I. d.o.o, 1000: Ljubljana, Slovenia, 2002.

[78] Ghodhbani, and E. Haj Taïeb, "Numerical coupled modelling of water hammer in quasi-rigid thin pipes", Proceedings of the Fifth International Conference Design and Modeling of Mechanical Systems (CMSM), Tunisia pp. 253-264, 2013.
[http://dx.doi.org/10.1007/978-3-642-37143-1_31]

[79] A.R. Simpson, and A. Bergant, "Numerical comparison of pipe-column-separation models", *J. Hydraul. Eng*., vol. 120, no. 3, pp. 361-377, 1994.
[http://dx.doi.org/10.1061/(ASCE)0733-9429(1994)120:3(361)]

[80] A.S. Tijsseling, "Exact solution of linear hyperbolic four-equation system in axial liquid-pipe vibration", Journal of Fluids and Structures, vol. 18, no. 2, pp. 179-196, 2003.
[http://dx.doi.org/10.1016/j.jfluidstructs.2003.07.001]

[81] A.S. Tijsseling, Poisson-coupling beat in extended waterhammer theory.ASME Flow-induced vibration and noise., Department of Civil Engineering, University of Dundee: Dundee, United Kingdom, Vol. 53-2, pp. 529-532, 1997.

[82] A.Bergant, and A.R. Simpson, "Pipeline column separation flow regimes", *J. Hydraul. Eng*., vol. 125, no. 8, pp. 835-848, 1999.
[http://dx.doi.org/10.1061/(ASCE)0733-9429(1999)125:8(835)]

[83] W. Wagner, and H.J. Kretzschmar, International steam tables., 2nd ed. Springer: Germany, 2008.
http://dx.doi.org/10.1007/978-3-540-74234-0

[84] D.C. Wiggert, F.J. Hatfield, and S. Stuckenbruck, "Analysis of liquid and structural transients by the method of characteristics", *J. Fluids Eng*., vol. 109, no. 2, pp. 161-165, 1987.
[http://dx.doi.org/10.1115/1.3242638]

[85] A.G.T.J. Heinsbroak, and A.S. Tijsseling, "The influence of support rigidity on water hammer pressures and pipe stresses", In: Proc. 2nd Int. Confer. Water Pipeline Systems: Edinburgh, UK, 1994, pp. 17-30, 1994.

[86] S. Kaneko, Flow-induced vibrations classifications and lessons from practical experiences., 2nd ed Elsevier, 2014.

[87] A.E. Vardy, and JM.B. Brown, "Transient turbulent friction in smooth pipe flows", In: Journal of Sound and Vibration, Civil Engineering Department, University of Dundee, Dundee DD1 4HN, Elsvier: Scotland, UK, 259(5), pp. 1011-1036, 2003.

http://dx.doi.org/10.1006/jsvi.2002.5160

[88] A.E. Vardy, and JM.B. Brown, "Transient turbulent friction in fully-rough pipe flows", In: Journal of Sound and Vibration Civil Engineering Department, School of Engineering, University of Dundee, Elsvier: Dundee DD1 4HN, UK, 270, pp. 233-257, 2004. [http://dx.doi.org/10.1016/S0022-460X(03)00492-9]

[89] A.Ghodhbani, "Modelling and Simulation of transient cavitation in pipelines", In: Thesis report, National Engineering School of Sfax, Tunisia, 2021.

[90] W. Zielke, "Frequency-dependent friction in transient pipe flow", ASME J. Basic Eng, series D, vol. 91, no. 4, 1969.

[91] A.Adamkowski, and M. Lewandowski, "Experimental examination of unsteady friction models for transient pipe flow simulation", *J. Fluids Eng*., vol. 128, no. 6, pp. 1351-1363, 2006. [http://dx.doi.org/10.1115/1.2354521]

[92] J. Vítkovský, "Efficient and accurate calculation of zielke and vardy-brown unsteady friction in pipe transients", S.J. Murray, Ed., Proceedings of the 9th International Conference on Pressure Surges, pp. 405-419, 2004.

SUBJECT INDEX

E

F

G

H

I

J

K

L

M

N

O

P

R

S

T

V

W

Abdelaziz Ghodhbani

Prof. Abdelaziz Ghodhbani is teaching mechanical engineering at the Higher Institute of Technology of Sidi Bouzid, Tunisia. He started his research after his master's degree from the National Engineering School of Sfax (NESS), Tunisia in 2009. He has been a member of the Laboratory of Applied Fluid Mechanics, Process Engineering and Environment (Lab. AFMPEE) at the NESS. In 2021, he obtained his doctorate in mechanical engineering from the NESS. He is a member of the fluid mechanics work team of the Lab. AFMPEE, and his work is focused on cavitation in turbomachines.

Mohsen Akrout

Prof. Mohsen Akrout serves as a professor of mechanical engineering at the National Engineering School of Sfax (NESS). He is a graduate of the National Institute of Applied Sciences (INSA Lyon, France). He is an internal quality auditor specialized in the implementation of quality management systems (ISO 9001 Certification). He is also a consultant and advisor to companies for the organization of their management systems and the optimization of their production flows. He is a member of the fluid mechanics work team of the Lab. AFMPEE and he focuses his work on production and quality management, organization and optimization of processes and numerical modeling.

Sami Elaoud

Prof. Sami Elaoud serves at National Engineering School of Sfax (NESS), Tunisia. He obtained the Ph.D. and HDR degrees in mechanical engineering from the NESS in 2009 and 2015, respectively. From 1990 to 2009, he worked in several industrial companies such as, Polina-Tunisa and Schlumberger-Dowell-International Company. He joined the Tunisian University in 2009, as an assistant professor and was promoted to associate professor in 2016. His domain of interest is fluid mechanics, fluid structure interaction, numerical modeling of flows inside centrifugal pumps and complex systems. He is the head of the fluid mechanics work team team of the Lab. AFMPEE.